Spring 5-15-2018

Transcriptional Regulation of Arrhythmia: from Mouse to Human

Yun Qiao
Washington University in St. Louis

WASHINGTON UNIVERSITY IN ST. LOUIS

School of Engineering and Applied Science
Department of Biomedical Engineering

Dissertation Examination Committee:
Stacey Rentschler, Co-Chair
Igor R. Efimov, Co-Chair
Nathaniel Huebsch
Colin Nichols
Jonathan Silva

Transcriptional Regulation of Arrhythmia: from Mouse to Human

by

Yun Qiao

A dissertation presented to
The Graduate School
of Washington University in
partial fulfillment of the
requirements for the degree
of Doctor of Philosophy

May 2018
St. Louis, Missouri

Table of Contents

List of Figures

List of Abbreviations

SSS	Sick sinus syndrome
AF	Atrial fibrillation
GWAS	Genome-wide association studies
CV	Conduction velocity
APD	Action potential duration
SAN	Sinoatrial node
AVN	Atrioventricular node
ECG	Electrocardiography
IIR	Infinite impulse response
FIR	Finite impulse response
AERP	Atrial effective refractory period
SNRT	sinus node recovery time
cSNRT	corrected sinus node recovery time
SVT	supraventricular tachycardia
NICD	Intracellular domain of Notch protein
iNICD	Inducible Notch intracellular domain
HR	Heart rate
CT	Crista terminalis
PDMS	polydimethylsiloxane
RA	Right atrium
Nkx2-5	NK2 homeobox 5
Cx40	Connexin 40
SVC	Superior vena cava
IVC	Inferior vena cava

Hrt1	Hairy-related transcription factor 1
Hes1	Hairy and Enhancer of Split-1
GUI	Graphic user interface
Pt/Ir	Platinum-iridium

Acknowledgments

First and foremost, I would like to thank my thesis advisor Dr. Igor Efimov and co-advisor Dr. Stacey Rentschler for their unwavering support and patient guidance during my PhD training. Dr. Efimov's abilities to "think big" and to push boundaries have fundamentally changed the way I tackle new challenges in both work and life. Dr. Rentschler's methodical approach to research has instilled in me an utmost respect for scientific rigor. Both Dr. Efimov and Dr. Rentschler demonstrate an unrelenting motivation and passion for science that I admire and aspire to. I feel truly fortunate to have had the opportunity to develop as a scientist and an engineer under their guidance.

I would also like to thank other members of my thesis committee, Dr. Nathaniel Huebsch, Dr. Colin Nichols, and Dr. Jonathan Silva. Their insights and feedback have been invaluable to my thesis research. I would also like to acknowledge Washington University for providing an exceptional academic and research environment. I would also like to thank Dr. Zhenyu Li for his support and guidance after my relocation with Dr. Efimov to the George Washington University.

In addition, I would like to thank all the past and current members of the Efimov lab, the Rentschler lab, the Li lab, and the Rogers lab that I have had the privilege of working with and learning from: Dr. Di Lang, Dr. Jacob Laughner, Dr. Sarah Gutbrod, Dr. Katherine Holzem, Dr. Matt Sulkin, Dr. Bas Boukens, Dr. Christopher Gloschat, Jaclyn Brennan, Dr. Kedar Aras, Dr. Sharon George, Dr. Rokhaya Faye, Dr. Benjamin Lee, Dr. Alejandro Murillo, Rose Yin, Anna Gams, Dr. Haytham Aly, Dr. Aditi Chiplunkar, Dr. Ben Gillers, Rich Li, Dr. Seung-Kyun Kang, Dr. Jahyun Koo, and Dr. Philipp Gutruf. I would like to thank the previous and current lab managers of the Efimov lab and the Rentschler lab, Megan Flake, Aaron Koppel, Stephanie

Hicks, and Christian Miccile. A specially thanks to Catherine Lipovsky, a dear friend who I share the co-first authorship with on my first publication, without her dedication to science the work would not have been possible. I would also like to extend a special thanks to Baichen Li and Quan Dong, for their significant technical support to my research, the critical discussion of the project, and for tirelessly answering all of my questions. This dissertation would not have been possible without the help of all the undergraduate and master research assistants that I have had the pleasure of working with: Sofian Obaid, Christian Miccile, Trisha Talapatra, Zexu Lin, Sihui Li, and Kailin Baechle. They have made me a better scientist and teacher. I also want to especially thank Chaoyi Kang, my experiment partner for four years and one of my best friends, for always being there even during the late hours.

I would like to thank my parents, for their unconditional love and support. Words cannot express my gratitude to them for all the sacrifices that they have made for me. Finally, I would like to express my deepest gratitude to my wife, Jing Zhang, for being my best friend and the best partner in life I could have ever dreamed of for the last 9 years.

Yun Qiao

Washington University in St. Louis

May 2018

To my wife Jing

and my parents Qingli and Guoqiang

for your unconditional love, support, and encouragement

Abstract of the Dissertation

Transcriptional Regulation of Arrhythmia: from Mouse to Human

by

Yun Qiao

Doctor of Philosophy in Biomedical Engineering

School of Engineering and Applied Science

Washington University in St. Louis, 2018

Professor Igor R. Efimov, Thesis Advisor

Professor Stacey Rentschler, Thesis Co-Advisor

In the last two decades, our understanding of cardiac arrhythmias has been accelerated immensely by the development of genetically engineered animals. Transgenic and knockout mice have been the "gold standard" platforms for delineating disease mechanisms. Much of our understanding of the pathogenesis of atrial and ventricular arrhythmias is gained from mouse models that alter the expression of specific ion channels or other proteins. However, cardiac arrhythmias such as atrial fibrillation are heterogeneous diseases with numerous distinct conditions that could not be explained exclusively by the disruption of ionic currents. Increasing evidence suggests disruption of signaling pathways in the pathogenesis of cardiac arrhythmias. Although crucial for studying disease mechanisms, animal models often fail to predict human response to treatments due to inter-species genetic and physiological differences. Cardiac slices obtained from human hearts have been demonstrated as an accurate model that more faithfully recapitulates human cardiac physiology. However, the use of the human cardiac slices for evaluating the transcriptional regulation of arrhythmia is hampered by tissue remodeling and dedifferentiation in long-term culture of the slices.

The first part of this dissertation aims to elucidate one of the potential mechanisms of sick sinus syndrome and atrial fibrillation induced by transient reactivation of Notch, a critical transcription factor during cardiac development and has been shown to be reactivated in the adult heart following cardiac injury. When Notch is transiently reactivated in the adult mice to mimic the injury response, the animals exhibits slowed heart rate, increased heart rate variability, frequent sinus pauses, and slowed atrial conduction. The electrical remodeling of the atrial myocardium results in increased susceptibility to atrial fibrillation. The transient reactivation of Notch also significantly altered the atrial gene expression profile, with many of the disrupted genes associated with cardiac arrhythmias by genome-wide association study.

The second part of this dissertation aims to address the lack the translation from animal research to human therapies by extending the human cardiac slice viability in culture. With the optimized culture parameters, human cardiac slices obtained from the left ventricular free wall remained electrically viable for up to 21 days *in vitro* and routinely maintained normal electrophysiology for up to 4 days. To genetically alter the human cardiac slices, a localized gene delivery technique was evaluated and optimized.

The third part of the dissertation aims to further improve long-term culture of human cardiac slices and to increase the availability of human tissue for research by developing a self-contained heart-on-a-chip system for automated culture of human cardiac slices. The system maintains optimal culture conditions and provides electrical stimulation and mechanical anchoring to minimize tissue dedifferentiation. The work allows for accelerated optimization of long-term culturing of human cardiac slice, which will enable study of arrhythmia mechanisms on human cardiac tissue via targeted control of transcription factors.

Chapter 1: Introduction

With the earliest description tracking back to ancient Egypt, Greece, and India, heart disease has been observed and studied for centuries (Davis, Hobbs, & Lip, 2000). However, heart disease still remains the leading cause of death for both men and women in the United States. Annually in the US, about 610,000 people die of heart disease, which accounts for approximately 1 in every 4 deaths (CDC. NCHS., 2015). Cardiac arrhythmia is a significant cause of morbidity and mortality, and it increases in prevalence with aging, such that 15 percent of the population older than 70 years of age suffers from arrhythmia (Psaty et al., 1997). Elucidating the pathogenesis of cardiac arrhythmia is crucial to developing effective treatments. This dissertation is focused on delineating a potential mechanism of sick sinus syndrome caused by disrupted transcriptional regulation following cardiac injury, and development of a novel platform using human cardiac tissue for long-term studies of drugs, exogenous gene expression, and transcriptional regulation.

1.1 Cardiac slice as a model of the heart

Research in experimental cardiac electrophysiology has been primarily limited to animal models such as mice, rabbits, dogs, minipigs, and zebrafish (Kaese et al., 2013). Few studies have collected electrophysiological measurements from the human heart due to the difficulty in obtaining and maintaining electrically viable tissue samples, and lack of reliable model systems of the human myocardium (de Boer, Camelliti, Ravens, & Kohl, 2009). Vibratome-cut human cardiac slices have recently emerged as a model for electrophysiological and pharmacological

testing due to its advantages over existing models (Brandenburger et al., 2012; Camelliti et al., 2011; Habeler, Peschanski, & Monville, 2009). When compared with iPSC-derived myocytes, human cardiac slices more faithfully replicate adult human cardiac electrophysiology with a mature myocyte phenotype. When compared with isolated human myocytes, cardiac slices largely preserve the natural extracellular environment and coupling with the surrounding myocytes, helping to maintain the fully differentiated phenotype. Maintenance of the native tissue context is especially important for testing human gene therapy approaches. When compared with human ventricular wedge preparations, cardiac slices do not require intact human ventricles and can be obtained from small biopsy samples. Most importantly, human cardiac slices can be prepared at a thickness around the diffusion limit of oxygen, thus allowing them to be cultured long-term for studying drug exposure and gene modulation (Brandenburger et al., 2012; Bussek et al., 2012).

Despite wide adaptation of tissue slices obtained from brain, kidney, liver, lung, and pancreas, reliable methods of producing viable cardiac slices have only been developed only recently due to the elasticity of the myocardium making it difficult to cut the tissue without deforming it (Bussek et al., 2009). Most of the published electrophysiological measurements on cardiac slice have been recorded using single cell microelectrode techniques or 60 channel multi-electrode array (MEA) systems (Brandenburger et al., 2012; Bussek et al., 2009, 2012; Camelliti et al., 2011). Few studies on cardiac slices have utilized high resolution optical mapping to characterize the conduction parameters of the cardiac slices (Kang et al., 2016; Wang et al., 2015).

When cut at less than 400 μm, sufficient tissue oxygenation occurs by diffusion, allowing the maintenance of tissue viability in culture (Brandenburger et al., 2012; Bussek et al., 2012;

Kang et al., 2016). Cardiac slices obtained from neonatal rat hearts have maintained long-term viability in culture for up to 3 months (Habeler, Pouillot, et al., 2009). However, to enable modeling of adult physiology and pathology, cardiac slices obtained from adult hearts would be a better model system. With conventional culture techniques that do not electrically stimulate the tissue, long-term culture of adult cardiac slices can result in altered electrophysiology due to myocyte dedifferentiation. A study using adult rat cardiac slices showed increasing level of apoptosis proportional to the number of days in culture (Kaneko, Coppen, Fukushima, Yacoub, & Suzuki, 2012). Gap junctions, which are composed of connexin proteins, play a large role in the propagation of electrical impulses in the heart. Immunolabeling and Western blots for connexin 43 (*Cx43*) revealed reduction in protein expression after just one day in culture, with undetectable *Cx43* expression after 6 days in culture. Reduction in connexin protein would directly affect conduction velocity (CV) and excitability of the tissue.

Previous reports of organotypic culture of ventricular slices obtained from adult mammalian hearts mostly have been limited to 48 hours, and have observed a slightly prolonged AP duration, while other conduction parameters remained stable (Bussek et al., 2012). One group has been able to demonstrate viability of adult human ventricular slices for up to 28 days in culture (Brandenburger et al., 2012). After 28 days, the majority of cultured slices demonstrated normal electrophysiological responses to pharmacological tests, but exhibited significant tissue remodeling during culture. Hematoxylin and eosin (H&E) stain revealed loss of normal sarcomeric structures and actinin distribution. Expression of transcripts encoding the major ion channel subunits Cav1.2, Nav1.5, and NCX remained stable in the cultured slices. However, the cultured slices exhibited some electrophysiological changes such as triangulation of the action potential and reduction in CV.

Electrical stimulation has been shown to maintain structural and functional properties of isolated adult rat ventricular myocytes (Folliguet et al., 2001). In the field of tissue engineering of cardiac and skeletal muscles, biomimetic culture conditions incorporating electrical and mechanical stimulation have been used to achieve greater maturity of myocytes differentiated from stem cells (Hirt et al., 2014; Lu et al., 2012; Maidhof et al., 2012; Tandon et al., 2009). Studies have shown that electrical stimulation of cardiomyocytes improved alignment, excitability and electrical coupling of the tissue (Rangarajan, Madden, & Bursac, 2014).

1.2 Cardiac arrhythmia mechanisms

Cardiac arrhythmia such as atrial and ventricular fibrillation are heterogeneous and multifaceted diseases. On the most fundamental level, atrial and ventricular fibrillation is caused by reentry, an abnormal propagation of electrical activity in the myocardium. The concept of reentry was first described in 1913 by George Mines (Mines, 1913). Using a circular model of excitable tissue, Mines demonstrated that the slowing of conduction velocity and shortening of refractory periods creates a moving region of excitable tissue that permits reentry to occur (Fig. 1.1). Walter Garrey later published the "critical mass" theory based on his observation that size of the excitable tissue directly corresponds to reentry maintenance, and functional isolation of regions of the heart would stop the fibrillation. These observations paved the fundamental understanding of fibrillation mechanism and formed the basis for surgical dissection and ablation of the atria for atrial fibrillation (Cox, Schuessler, & Boineau, 2000).

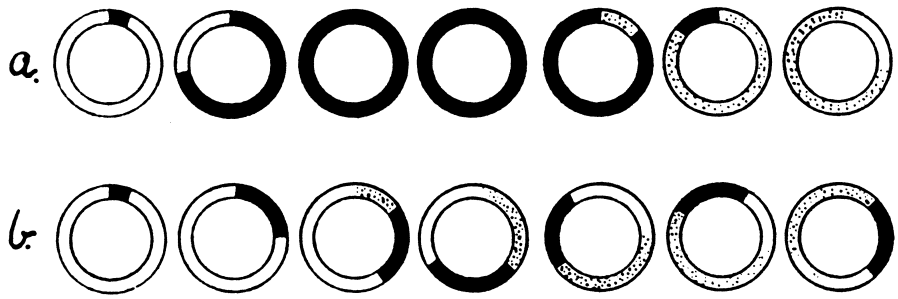

Figure 1.1 Mine's representation of reentry in a closed circuit of myocardium. A) A ring model of healthy excitable tissue with normal conduction velocity and refractory period. The black region presents tissue in absolute refractory. The shaded region represents tissue in relative refractory. The white region represents tissue in the excitable state. B) Abnormal tissue with slowed conduction, which allows time for the tissue to repolarize back to the resting state and permits the formation of reentry (Mines, 1913).

The "critical mass" theory was later explained by the concept of reentry wavelength by Thomas Lewis and mathematically depicted by Wiener and Rosenblueth (Lewis, 1925; Wiener & Rosenblueth, 1946), as shown in equation 1.1. Either slowing of conduction or shortening of effective refractory period would reduce the minimal wavelength required for sustained reentry. In the context of the "critical mass" theory, as the size of the excitable tissue approaches the wavelength of the tissue, the fibrillation is more likely to self-terminate.

$$\lambda = CV \times ERP \quad (1.1)$$

Equation for wavelength calculation, where λ is the wavelength, CV is conduction velocity of the excitable tissue, and ERP is effective refractory period of the tissue.

Action potential alternans are another major contributor of fibrillation, and often occurs at high heart rates. Instability of alternans can be predicted by examining the slope of action potential (APD) restitution curve. Created by measuring APD at incremental cycle length, APD restitution provides a holistic view on the repolarization process of the myocardium. When shortening the pacing cycle length, the reduction in APD is mostly contributed by incomplete

recovery of time-dependent potassium channels such as I_{Kr} and I_{Ks}. At shorter pacing cycle length when the diastolic interval (DI) is less than 100 ms, the APD is further reduced due to incomplete recovery of L-type calcium channel. When the diastolic interval is less than 40 ms, incomplete recovery of sodium channel indirectly shortens APD by reducing the amplitude of the action potential. The conduction velocity is also reduced at short cycle length due to the incomplete recovery of the sodium channel. Instability in alternans is promoted when the slope of the APD restitution curve is greater than 1. As demonstrated in Figure 1.2 C, the instability in alternans would grow and eventually result in functional block. When combined with CV restitution at short pacing cycle length, spatially discordant alternans could occur and result in local conduction block that give rise to reentry (Qu, Xie, Garfinkel, & Weiss, 2010).

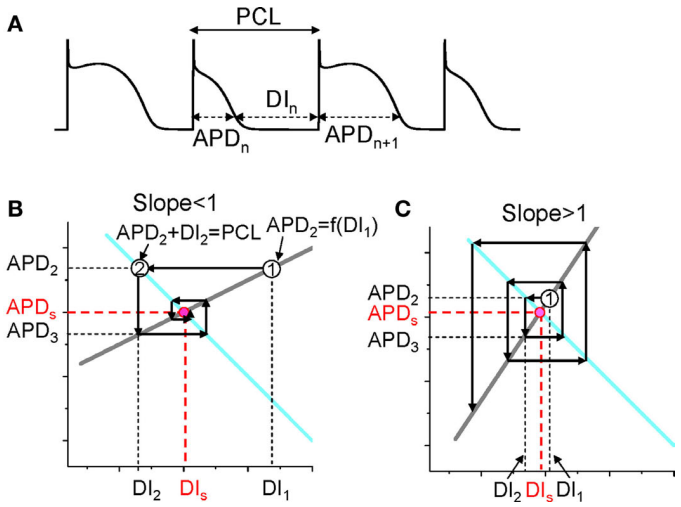

Figure 1.2 Instability in alternans promoted by steep APD restitution curve. A) An action potential trace illustrating action potential duration (APD), pacing cycle length (PCL), and diastolic interval (DI). B) Cobweb diagram showing the alternans stabilize when the slope of the APD restitution curve is less than 1. The grey line represents the APD restitution curve. The cyan line represent the relationship of PCL = APD + DI. C) Cobweb diagram showing that the alternans becomes unstable when the slope of the APD restitution curve is greater than 1 (Qu et al., 2010).

1.3 Optical mapping of the heart

Robust generation and propagation of the electrical impulses in the heart are crucial for cardiac function because of excitation-contraction coupling. Any abnormalities in cardiac electrophysiology can have profound adverse effects on the mechanical contraction of the heart(Lou, Fedorov, et al., 2011). Based on the principles of biophotonic imaging, optical mapping serves as an indispensable tool for studying cardiac electrophysiology by measuring membrane potential and intracellular calcium concentration.

As one of the most critical components of an optical mapping system, the photodetector must demonstrate exceptional sensitivity as well as sufficient spatial and temporal resolutions. As the name suggests, spatial resolution is how well the camera distinguish closely spaced features on the sample, and it depends on the number of pixels on the camera sensor and the field of view of the imaging system. Also referred to as the sampling rate, temporal resolution defines the camera's ability to capture fast occurring events. Greater signal to noise ratio can be achieved at the expense of lower sampling rate, which allows more photons to hit the sensor during each frame. Alternatively, increasing the pixel size of a photodetector improves the low-light performance and temporal resolution of a camera sensor by allowing for more photons to be captured by each pixel. However, assuming the total size of the photodetector remains the same, enlargement of the individual pixels would result in a lowered pixel density and reduced spatial resolution. Some of the camera sensors available today include charge coupled device (CCD), complementary metal-oxide semiconductor (CMOS), and photodiode array (PDA) (Efimov, Nikolski, & Salama, 2004). Each sensor technology has its own tradeoffs between sensitivity, spatial and temporal resolution. The wide adaptation of CMOS sensors in consumer electronics

has expedited improvements in the CMOS sensors, which now offer the best of both worlds, demonstrating good spatial resolution combined with high temporal resolution.

Significant efforts have been invested into improving voltage-sensitive fluorescent indicators. To measure the cardiac action potential, voltage-sensitive probes such as RH-237 and di-4-ANEPPS are commonly used. As the membrane potential changes, the voltage-sensitive probes bound to the cell membrane undergo conformation change, which result in a redshift in emission peak. However, these voltage-sensitive probes suffer from low signal-to-noise ratio (SNR), since the peak fluorescence intensity only changes by less than 5% during recording (Efimov et al., 2004). The problem of low SNR of the probes is circumvented by measuring the shift in emission spectrum rather than the change in peak fluorescence intensity at a fixed wavelength, by using a long-pass filter to measure the changes in total fluorescence intensity (Lang, Sulkin, Lou, & Efimov, 2011).

1.4 Dissertation objective and scope

With numerous distinct underlying conditions, cardiac arrhythmia cannot be faithfully recapitulated in transgenic animal models that alter selective ion channels. Disruption in the transcriptional signaling pathways has been implicated in the pathogenesis of arrhythmia. The objective for the first part of this dissertation is to delineate one of the potential mechanisms of sick sinus syndrome and atrial fibrillation induced by transient reactivation of Notch, a critical transcription factor during cardiac development and has been shown to be reactivated in the adult heart following cardiac injury. The extensive evaluation of the Notch-induced sick sinus syndrome model was made possible by significant contribution of two co-first authors. In

Chapter 2, I present the disease model, explain the experimental and analysis techniques used, and elucidate the altered electrophysiology and increased arrhythmia susceptibility.

Due to difficulties of translation from animal research to human therapies, the objective for the second part of this dissertation is to bridge the gap between bench research and human clinical therapy by extending the human cardiac slice viability in culture and optimizing viral transduction techniques. In Chapter 3, I present an optimized culture protocol with which human cardiac slices obtained from the left ventricular free wall remained electrically viable for up to 21 days *in vitro* and routinely maintained normal electrophysiology for up to 4 days.

To further improve human cardiac slice culture for long-term studies, the objective for third part of the dissertation aims to develop a self-contained heart-on-a-chip system for automated culture of human cardiac slices. In Chapter 4, I present a culture system that maintains optimal culture conditions and provides electrical stimulation and mechanical anchoring to minimize tissue dedifferentiation. This work allows for accelerated optimization of long-term culturing of human cardiac slice, which will enable study of arrhythmia mechanisms on human cardiac tissue via targeted control of transcription factors.

Chapter 2: Transient Notch activation induces long-term gene expression changes leading to sick sinus syndrome in mice

Cardiac arrhythmias are a significant cause of morbidity and mortality with increasing prevalence with aging, such that 15 percent of the population older than 70 years of age suffers from arrhythmias (Psaty et al., 1997). Genome-wide association studies (GWAS) have associated sick sinus syndrome (SSS) and atrial fibrillation (AF) with mutations in Nkx2-5, a transcriptional factor that controls gene regulatory networks of the heart (Marsman, Tan, & Bezzina, 2014). Conditional knockout of Nkx2-5 in the atrial myocardium leads to global activation of Notch, a critical regulator of cardiac morphogenesis (Nakashima et al., 2014). Therefore, we aimed to study effects of Notch activation on atrial electrical remodeling. Though it is normally not expressed within adult myocardium, Notch is transiently reactivated in the heart following cardiac injuries (Gude et al., 2008; Li, Hiroi, & Liao, 2010; R. Zhang et al., 2013). Here, we developed a mouse model to study the effects of transient Notch activation on electrical remodeling and cardiac arrhythmias. We found that transient Notch activation in the adult heart disrupted expression of major regulators of conduction, which resulted in altered atrial electrophysiology, including sinus bradycardia, sinus pauses, slowed atrial conduction, and increased susceptibility to atrial fibrillation. Many of the misregulated genes have been associated with sinus bradycardia and AF susceptibility (Van Den Boogaard, Barnett, & Christoffels, 2014).

2.1 Introduction

The normal rhythmic activation of the heart is governed by an intricate network of different types of cardiomyocytes. Each subpopulation of myocytes has unique electrical characteristics due to their different composition of ion channels. Atrial and ventricular working myocytes have a more hyperpolarized resting action potential with fast upstroke velocity, whereas sinus and atrial-ventricular nodal myocytes have a more depolarized resting membrane potential with slower upstroke velocity (Park & Fishman, 2011). Understanding the transcription factors that control the electrophysiological patterning of the heart has important clinical significance. Reactivation of these factors may have physiological benefits in treating cardiac diseases through regenerative medicine. On the other hand, unintended activation of some factors may disrupt normal conduction parameters within the heart, making the tissue more susceptible to arrhythmias (Rentschler et al., 2011).

Mutations in non-coding regions near SCN5A have been linked with high AF susceptibility in GWAS (Van Den Boogaard et al., 2014). Our preliminary results using a genetically engineered murine model to induce Notch within the myocardium demonstrate reduced *Scn5a* expression in Notch activated hearts. This suggests that Notch-mediated reprogramming could alter the epigenetic regulation of the genes associated with arrhythmias. Thus, studying the electrical remodeling following Notch activation is important to further the understanding of the underlying electrophysiological mechanisms of arrhythmias.

2.1.1 Role of Notch during cardiac development

Notch has been shown to be an essential transcription factor regulating development of the heart (Rentschler et al., 2011). Activation and inactivation of Notch during development led to dramatically different outcomes. Transgenic mice with Notch inactivation had hypoplastic atrioventricular node (AV) nodes, which manifested as shortening in AV delay during activation of the heart. On the other hand, mice with Notch ectopically expressed within the atrioventricular region during development exhibited ventricular pre-excitation caused by the presence of accessory pathways in the annulus fibrosis. These mice were also more susceptible to atrial tachycardias during programmed stimulation (Rentschler et al., 2011).

2.1.2 Notch-induced reprogramming following organ injury

Cardiac injury has been shown to cause the activation of Notch in the heart of adult mouse and zebra fish (Gude et al., 2008; Li et al., 2010; R. Zhang et al., 2013). However, the effects on conduction parameters and arrhythmias have not been well characterized. On the other hand, studies of Notch activation after liver damage have been well characterized (Yanger et al., 2013). Injury in the liver tissue causes Notch activation that initiates a reprogramming cascade that reprograms hepatocytes to biliary cells. Studying the effect of Notch-mediated reprogramming may provide insights to the cause of increased instances of arrhythmias after myocardial infarction in human.

2.2 Methods

2.2.1 Generation of transgenic mice

αMHC-rtTA and *tetO_NICD* mice were mated to obtain *αMHC-rtTA; tetO_NICD* mice in which the expression of NICD could be turned on by feeding the animal with doxycycline chow. To model the adult activation of Notch, the tet-on system is used to activate Notch in myocytes after birth. Mice between the ages of 2-5 months were used in the experiment. To compensate for the possibility of a doxycycline effect, *αMHC-rtTA* mice on doxycycline were used as the control animals in the functional studies. For the experimental group, age-matched *αMHC-rtTA*; *tetO_NICD* littermates on doxycycline were used. All animal protocols were approved by the Institutional Animal Care and Use Committee at Washington University in St. Louis.

2.2.2 ECG recordings

To track the long-term changes in heart rate, electrocardiography (ECG) recordings were performed on conscious and anesthetized mice. A physical restrainer with built-in electrodes (ECG Tunnel, EMKA Tech) was used for performing ECG recordings on conscious mice. Heart rate was calculated from ECG segments with at least 100 identifiable beats. To perform ECG recording on anesthetized mice, the animals were anesthetized with 2% isoflurane. Heart rate was averaged from the first minute of ECG recordings. For evaluating the diurnal heart rate cycle, heart rate variability, and sinus pauses, telemetry studies were performed on mice between 3-5 months of age from the start of the doxycycline treatment. ETA-F10 implantable radio frequency transmitters (Data Sciences International Inc.) were implanted subcutaneously for lead II ECG recordings. After one week of post-operative recovery, baseline recording was obtained

before the animals were introduced to the doxycycline chow. Ambulatory ECG was recorded while the animals were free moving in cages. 4 minutes of recording was taken every hour at 2 kHz sampling rate for 4 weeks.

2.2.3 Telemetric ECG analysis

Custom MATLAB algorithms were developed to analyze the telemetric ECG recorded on the control and Notch-activated mice. The raw ECG recordings were structured before being conditioned for R wave detection. The signal conditioning process involves a band-pass infinite impulse response (IIR) Butterworth filter for removing baseline drift, electrical noise, and electromyogram signal. A notch filter was implemented to remove the 60Hz interference. The amplitude of the ECG was then normalized before implementing peak detection based on the R wave amplitude and minimal rejection time interval. The timing of the identified R waves was used for calculating heart rate, heart rate variability, and episodes of sinus pauses. Pincaré plots were generated by comparing adjacent RR intervals.

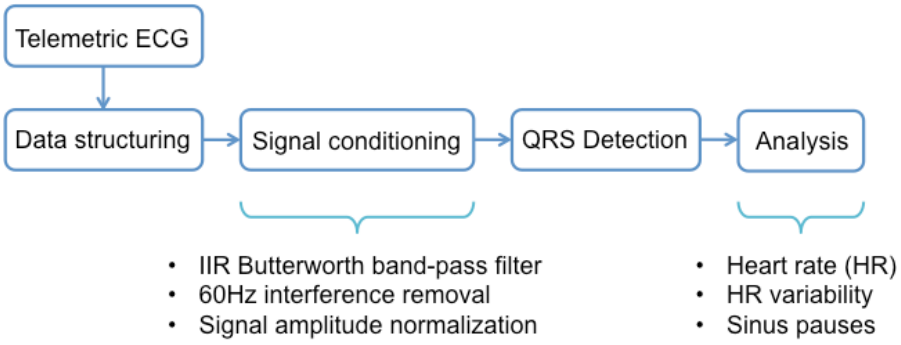

Figure 2.1 Telemetric ECG analysis pipeline.

2.2.4 Optical mapping of Langendorff-perfused murine hearts

Optical mapping experiments were conducted to study the electrical conduction parameters of the murine hearts. A CMOS camera system was used to detect changes in the membrane potential of Langendorff-perfused murine hearts stained with Di-4-ANEPPS, a voltage-sensitive dye. The cardiac tissue was kept viable using perfusion with Tyrode's solution at 37°C with the pH maintained at 7.4. Blebbistatin, an excitation-contraction uncoupler, was perfused to the tissue to eliminate motion artifacts in the recorded optical signal. A green LED light source with the wavelengths of 520 ± 5 nm was used to excite the voltage-sensitive dye. The emitted fluorescence was filtered by a long-pass filter at 650 nm and collected by the CMOS camera.

2.2.5 Analysis of optical action potential

The recorded data was analyzed using an open source custom MATLAB program. Using the spatial coordinates and time of the maximum derivatives (dV_m/dt_{max}) of the optical action potentials, activation maps of the cardiac tissues was generated. To filter out undesirable fluorescent scattering from the ventricles, a mask of the atria was created based on the maximum fluorescence intensity during atrial activation. The activation maps were used to calculate the conduction velocity. Action potential duration of the atria was calculated by taking the time difference between depolarization and 80% repolarization of the optical action potentials and averaged. Since the conduction velocity and action potential duration are rate-dependent, optical mapping recordings were conducted when the atria was paced at 100ms pacing cycle length.

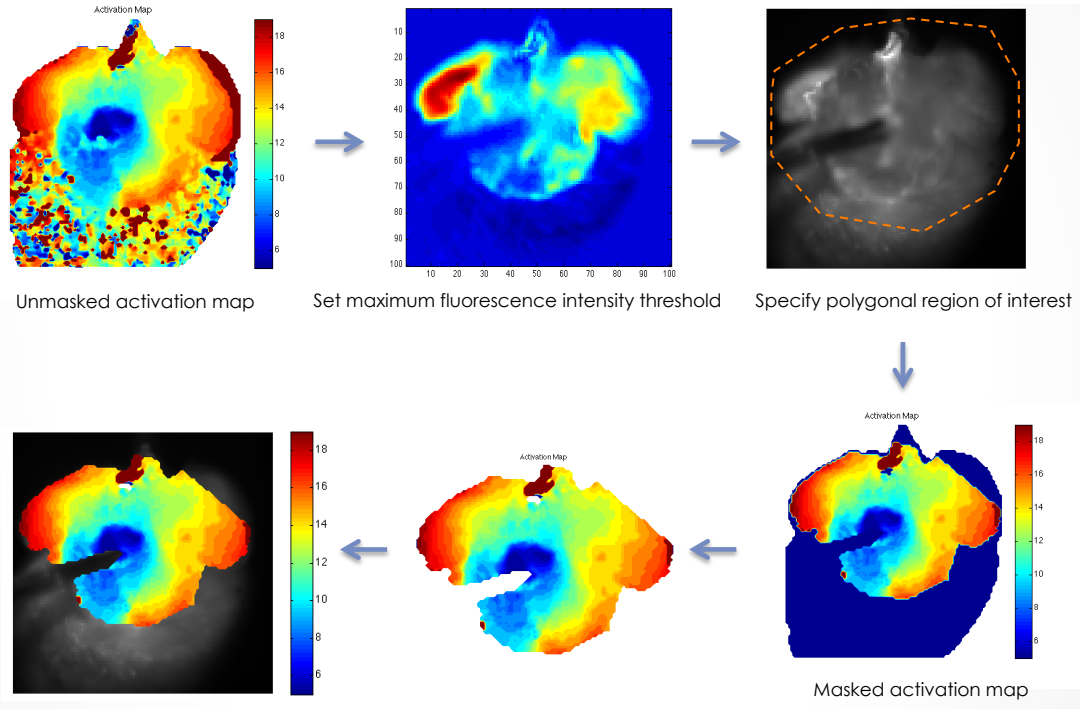

Figure 2.2 Filtering of atrial optical action potential.

2.2.5 Conduction velocity analysis

As one of the key electrophysiological parameters of the heart, conduction velocity provides insights into the health of the myocardium. Conditions such as ischemia, fibrosis, and altered cell coupling can result in significant reduction in conduction velocity (KLEBER, 2004). Although conduction velocity can be calculated by simply dividing the distance traveled by an activation wave front over a period of time, factors such as electrotonic conduction, curvature of the heart, and regions of conduction block significantly complicate the conduction velocity calculation. Two methods have been widely implemented to accurately calculate conduction velocity in optical mapping data. The local gradient method calculates the conduction velocity by average multiple local gradients of the activation times. However, insufficient spatial and temporal resolution of the optical mapping could result in overestimation of longitudinal

conduction velocity by the local gradient method (Doshi et al., 2015). With this method, it is also difficult to accurately calculate conduction velocity in tissue with conduction blocks. Doshi et al. proposed and developed a semi-automated method of calculating conduction velocity based on the single vector method. The semi-automated method allows users to accurately select regions of linear conduction at every angle to calculate the functional longitudinal and transverse conduction velocity (Fig. 2.3). This method was modified and implemented in this dissertation for calculating conduction velocity.

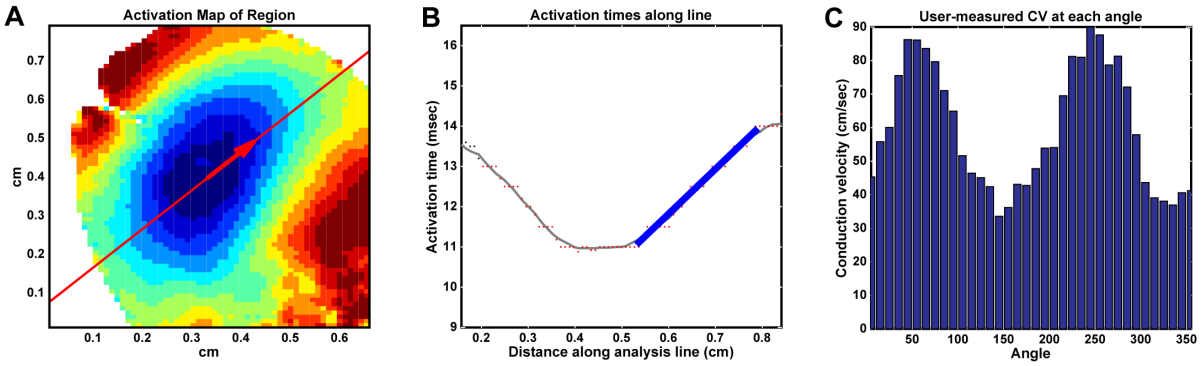

Figure 2.3 Longitudinal and transverse conduction velocity calculation. A) Activation map of mouse left ventricle during point pacing. Red line represents the line from which the activation times were extracted for conduction velocity calculation. B) Activation times (red dots) from the site of pacing along the red line in panel A. The thick blue line represents the linear region in the activation times from which the conduction velocity is calculated. C) Conduction velocity calculated at each angle from the site of pacing. The peaks represent the longitudinal conduction velocity, whereas the troughs represent the transverse conduction velocity.

2.2.6 Programmed stimulation for testing AF susceptibility

A programmed pacing protocol that consists of a series of single extrastimulus was performed on each heart. The stimulus amplitude used is twice the diastolic capture threshold with a pulse duration of 2 ms. For atrial single extrastimulus, a pacing drive train of 20 S1 at a

cycle length of 100 ms was used, followed by an S2 with a 50ms coupling interval, which was reduced in 5 ms intervals until loss of atrial capture (atrial effective refractory period, AERP). For sinus node recovery time determination (SNRT), a 15 second burst pacing at a cycle length of 100ms was used. The SNRT was defined as the interval between the last stimulus in the pacing train and the onset of first sinus return beat, and cSNRT (cSNRT) was calculated by subtracting the average RR interval from the SNRT. Episodes of supraventricular tachycardia (SVT) were defined as follows: rapid atrial activity faster than ventricular activity lasting greater than one second.

2.2.7 Arrhythmia analysis

Episodes of supraventricular tachycardia was recorded by optical mapping and analyzed using phase analysis. Phase analysis has been used for quantifying oscillating behavior in a chaotic signal. Extensive work has been done to validate the use of phase analysis for quantifying reentrant arrhythmias. Two out of phase periodic signals are required for calculating the phase. Hilbert transform was performed to create an analytical signal composed of a real and an imaginary component. In the case of arrhythmia analysis, the real component of the signal is the optical action potential during supraventricular tachycardia. The imaginary component of the analytical signal is the real component phase shifted by $-\pi/2$ in all frequencies. When plotted on the complex plane, the instantaneous phase is calculated by finding the angle between the analytical signal and the real axis.

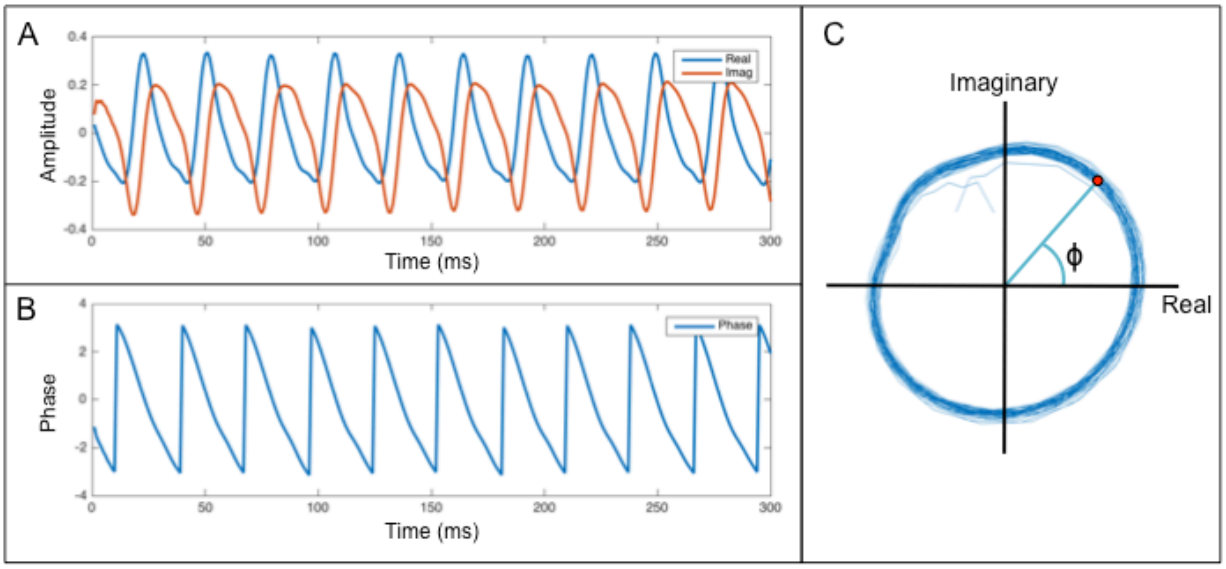

Figure 2.4 Phase analysis of optical action potential during AF. A) Optical action potential (blue) during AF and phase shifted signal (red) produced by Hilbert transform. B) Instantaneous phase calculated by finding the angle between the analytical signal and the real axis. C) Phase space plot showing how the instantaneous phase is calculated.

Phase maps were created by calculating the instantaneous phase for every pixel of the optical mapping data. The reentrant wavefronts were identified by regions with a phase of π/2. The centers of reentrant arrhythmias were identified as areas of phase singularities using the equation for calculating topological charge shown in equation 2.1. The phase singularities were calculated by convolving the phase gradients with the kernels shown in equations 2.2 and 2.3. The signs of the phase singularities represent the reentrant chirality.

$$n_t \equiv \frac{1}{2\pi} \oint_C \nabla\phi \cdot d\vec{l} = \pm 1 \tag{2.1}$$

$$\frac{1}{2\pi} \cdot (\nabla_x * k_y + \nabla_y * k_x) \tag{2.2}$$

$$\nabla_x = \begin{bmatrix} -\frac{1}{2} & 0 & +\frac{1}{2} \\ -1 & 0 & +1 \\ -\frac{1}{2} & 0 & +\frac{1}{2} \end{bmatrix}$$
$$\nabla_y = \begin{bmatrix} +\frac{1}{2} & +1 & +\frac{1}{2} \\ 0 & 0 & 0 \\ -\frac{1}{2} & -1 & -\frac{1}{2} \end{bmatrix} \quad (2.3)$$

2.2.7 Statistical analysis

All data are expressed as means ± standard error of the mean (SEM). Statistical analyses were performed after assessing for normal distribution using unpaired *t* tests with Welch's correction for comparison of 2 groups, and one-way ANOVA followed by a Dunnett's multiple comparisons test for comparison of 3 groups. Values of $P<0.05$ were considered statistically significant.

2.3 Results

Notch is a critical developmental regulator of morphogenesis, and normally it is not expressed in the adult heart (Rentschler et al., 2011). However, Notch is transiently reactivated in the adult heart following cardiac injuries (Gude et al., 2008; Li et al., 2010). GWAS have associated mutations in Nkx2-5 with SSS and AF susceptibility (Marsman et al., 2014). Conditional knockout of Nkx2-5 has been shown to lead to global activation of Notch signaling (Nakashima et al., 2014). We hypothesize that transient Notch reactivation may lead to electrical reprogramming, increasing susceptibility to sinus bradycardia and AF.

2.3.1 Transient reactivation of Notch leads to sinus bradycardia and frequent sinus pauses

To model the adult injury response, we utilized the Tet-on transgenic system to activate Notch signaling (iNICD) within adult murine myocardium (Corbel & Rossi, 2002). Notch signaling was transiently activated at 8 weeks of age for 3 weeks, followed by cessation of gene expression. This allows us to determine whether the observed electrical changes are stable in the absence of ongoing Notch expression, consistent with electrical reprogramming. ECGs and telemetry recordings were performed to measure heart rate and occurrences of sinus pause.

When compared with littermate controls, iNICD mice exhibited bradycardia. Significant differences in HR between control and iNICD mice are observed during conscious ECGs (778±20bpm vs 638±14bpm, p=3.6E-5), during ECGs performed under mild anesthesia (600±24bpm vs 462±17bpm, p=03.4E-4), and during telemetry recordings of free-moving mice (524±13bpm vs 448±27bpm, p=0.047) (Fig. 2.4 A). The ECG recordings demonstrate that the reduction in HR is largely due to prolongation in the R-R interval and not AV block (Fig. 2.4 B-C). When compared with the controls, iNICD mice also exhibit frequent sinus pauses (Fig. 2.4 C).

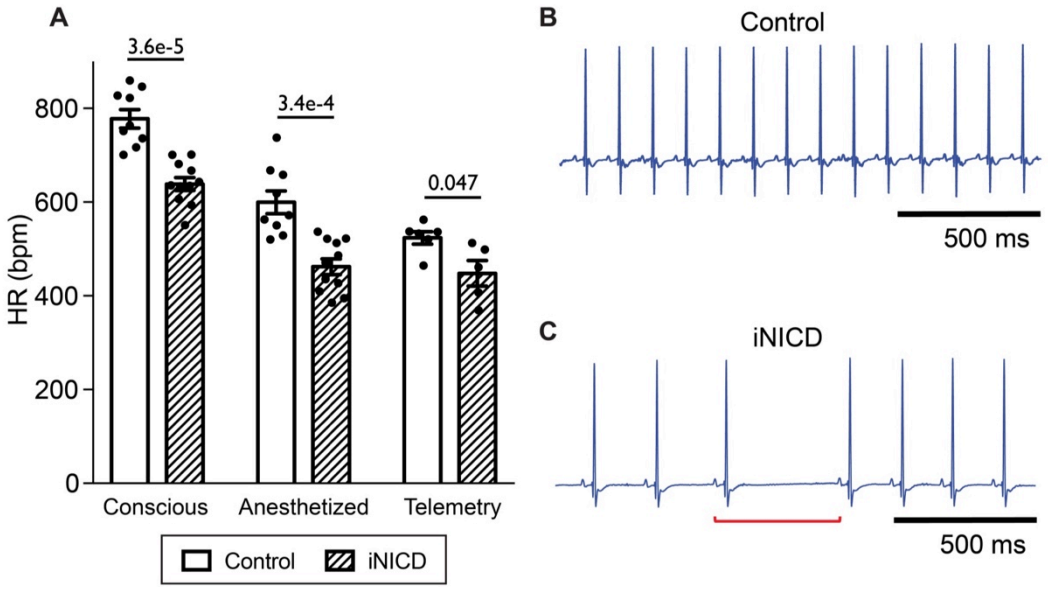

Figure 2.5 Transient reactivation of Notch leads to bradycardia and sinus pauses. A) Notch activated mice exhibited slowed heart rate. The values were calculated from ECG recordings taken from conscious, anesthetized mice, and from conscious telemetry monitoring. B) Telemetric ECG taken from a control mouse showing normal sinus rhythm. C) Telemetric ECG taken from a iNICD mouse showing slowed heart rate and an episode of sinus pause (highlighted by red bracket).

As a spatial summation of all electrical activities in the heart, ECG recordings are not able to identify the underlying mechanism of the observed sinus bradycardia and sinus pauses. Possible explanations include abnormal sinus node (SAN) automaticity, SAN exit block, intra-atrial conduction block, and abnormal innervation. To elucidate the mechanism underlying the slowed HR, analysis of the telemetric ECG was performed to evaluate the diurnal response of the mice. If the slowed HR phenotype observed in the iNICD mice is a result of abnormal innervation, the mice would be unresponsive to sympathetic stimulation and only exhibiting a lower HR during period of high activity at nighttime. As shown in Figure 2.5, the iNICD mice exhibited an overall slowed HR during both high activity and low activity with preserved diurnal heart rate response, suggesting normal autonomic innervation.

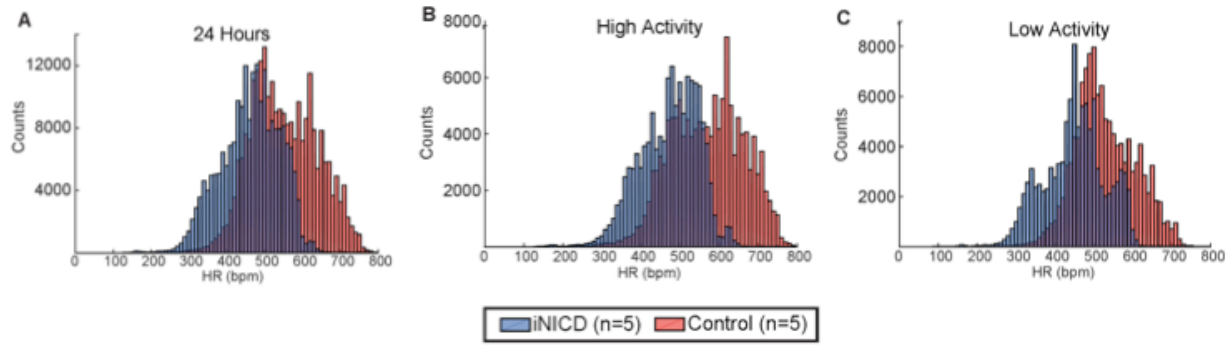

Figure 2.6 Preserved diurnal heart rate responses of iNICD mice. A) Heart rate distribution of control and iNICD mice over 24 hours. B) Heart rate distribution of control and iNICD mice during period of high activity from 6PM-6AM. C) Heart rate distribution of control and iNICD mice during period of low activity from 6AM-6PM. iNICD mice demonstrate preserved diurnal heart rate response, showing lower average heart rate during both daytime and nighttime.

In addition to the slowed HR phenotype, the iNICD mice also exhibited frequent episodes of sinus pauses, as observed in Figure 2.4 C. To quantify the sinus pauses, additional analysis were performed on the telemetry ECG recordings. Poincaré plot were generated to compare the RR interval of every beat with the RR interval of the subsequent beat. As shown in Figure 2.6A, the telemetry ECG recordings of a control animal produced a tight, linear cluster representing normal diurnal heart rate fluctuation with minimal beat-to-beat variation. On the other hand, the poincaré plot of an iNICD mice had a dispersed clustering, suggesting high HR variability and frequent sinus pauses. The average numbers of sinus pauses were summarized in figure 2.6C. When compared with the control animals, the iNICD mice exhibited significantly more episodes of sinus pauses, which are defined as beats with a RR interval that is 70% longer than the average baseline cycle length. Together, the sinus bradycardia, high heart rate variability, and frequent sinus pauses observed in the iNICD mice closely resembles manifestations of Sick sinus syndrome (SSS), also known as sinus node dysfunction.

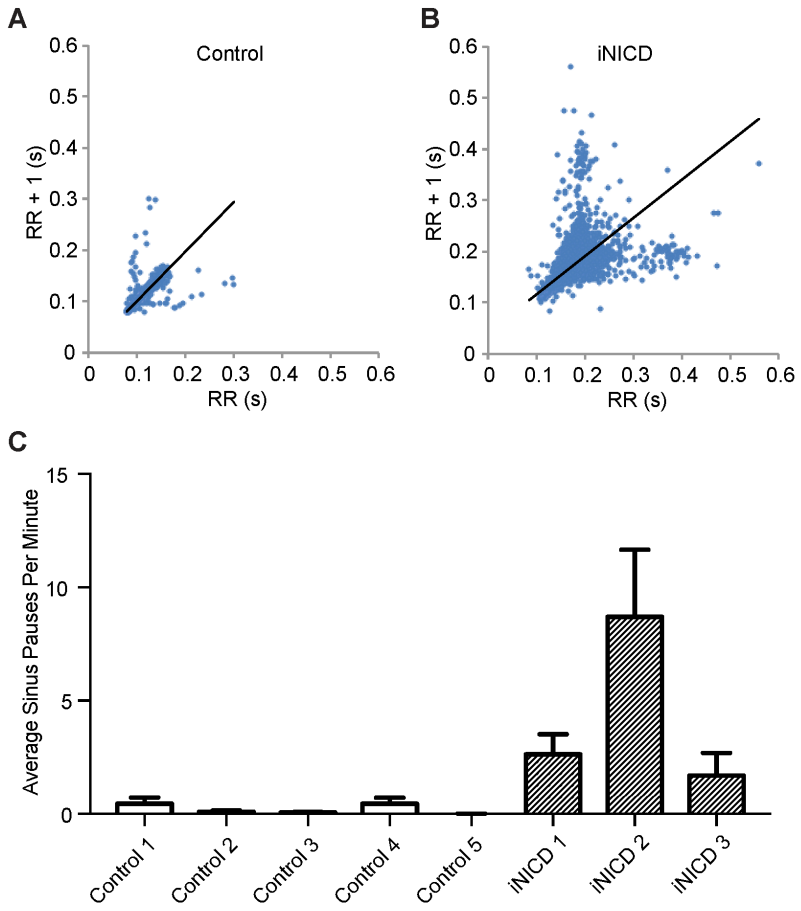

Figure 2.7 iNICD mice exhibit frequent sinus pauses. A) Poincaré plot of a control animal showing a stable heart rate response over 24 hours with minimal beat-to-beat variation. B) Poincaré plot of an iNICD mouse showing large beat-to-beat variation, which represents high heart rate variability and frequent sinus pauses. C). Analysis of telemetry ECG revealed that iNICD mice demonstrate significantly more episodes of sinus pauses when compared with the control animals.

2.3.2 Transient reactivation of Notch causes reduced atrial conduction velocity

To evaluate the extent of Notch induced electrical remodeling in the atrial myocardium, optical mapping and far-field ECG recording was performed on the Langendorff-perfused iNICD hearts and littermate controls. Under Langendorff perfusion and in the absence of sympathetic stimulation, the HR of the iNICD mice remained low, suggesting that the sinus bradycardia phenotype is not a result of altered autonomic response. Activation maps of the atria during sinus

rhythm were generated as shown in Figure 2.7A. When compared with the control atria, the iNICD atria exhibited slowed heart rate with 1:1 conduction from the SAN. The stable propagation of the electrical impulses from the SAN to the atrial myocardium in the iNICD atria excluded SAN exit block and intra-atrial conduction block as the mechanisms of the observed sinus bradycardia phenotype. Since conduction velocity (CV) and action potential duration (APD) are rate dependent. To accurately calculate the CV and APD of the isolated atria, activation of the atria were recorded via optical mapping under a constant stimulation at 100ms pacing cycle length. The activation maps revealed heterogeneous conduction and reduced conduction velocity in the right atrium (RA) of iNICD mice when compared with the controls (41.1±3.1cm/s vs. 29.0±1.8cm/s, p=0.02) (Fig. 2.7 B,D). The optical mapping experiments also revealed that the APD at 80% repolarization (APD_{80}) and the corrected sinus node recovery time (cSNRT) were unchanged, as shown in Figure 2.7 E,F. Compared with adult activation of Notch, Notch activation in juvenile mice at 3 weeks of age induced more severely altered electrophysiology. As shown in Figure 2.7 G, the optical mapping experiments revealed regions of the right atrium of the iNICD to be electrically quiescent during sinus rhythm. During electrical stimulation, the region of the right atrium remained electrically unexcitable, as shown in Figure 2.7 H.

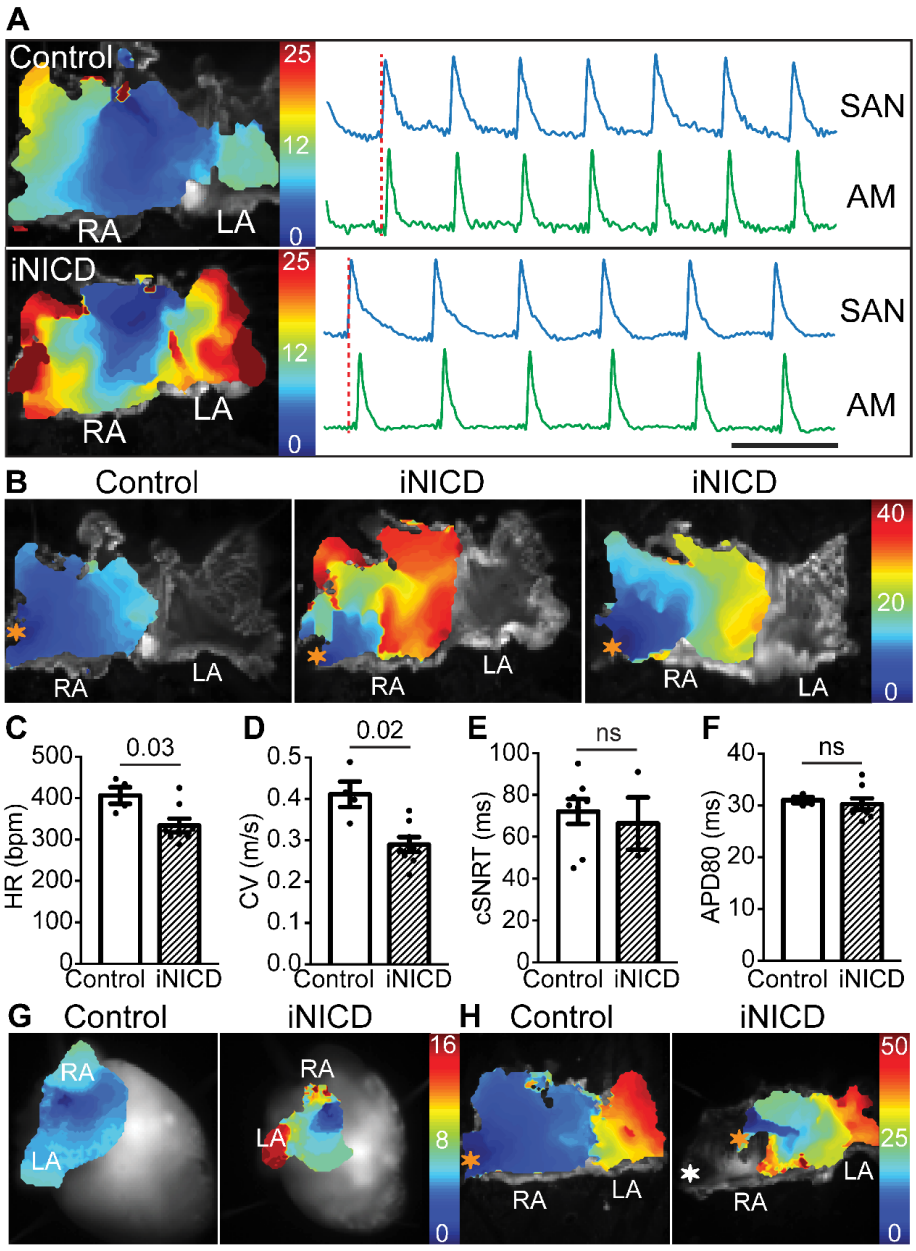

Figure 2.8 Transient Notch activation causes reduced atrial conduction velocity. A) Activation maps of isolated atria from a control and an iNICD mouse, showing 1:1 conduction from the sinus node. B) Activation maps of the right atria obtained from control and iNICD mice during constantly electrical stimulation for calculation of CV and APD. The activation maps of the iNICD animals show isochrones crowding and areas of conduction block. C) iNICD mice exhibit slowed heart rate when compared with the control under Langendorff perfusion. Optical mapping revealed slowed CV in iNICD mice (D), while APD and the corrected SAN recovery time (cSNRT) are preserved (E,F). G) Notch activation in juvenile mice at 3 weeks of age results in electrical silencing of a portion of the right atria during sinus rhythm. H) Electrical stimulation failed to capture the right atrial appendage (white asterisk).

2.3.3 Transient Notch activation result in persistent up-regulation of Notch target and prolonged bradycardia

Transient reactivation of the Notch signaling pathway in adult heart following cardiac injury has been previously demonstrated. To model the injury response, we utilized the tet-on system to transiently reactivated Notch in adult mice at eight weeks of age for various durations of doxycycline induction followed by washout periods of eight weeks to one year. Following three weeks of doxycycline induction, we observed a 7-fold increase in NICD expression and significant up-regulation of direct Notch target genes *Hrt1* and *Hes1* in the iNICD mice (Fig. 2.8 A, B). With a 2-day doxycycline induction followed by a one-year washout, NICD level returned to baseline as expected. In contrast, *Hes1* remained persistently up-regulated in the absence of on-going Notch expression (Fig. 2.8C). To evaluate the functional effect of the persistent up-regulation of *Hes1*, we tracked HR of iNICD mice with various induction periods, ranging from 12 hours to 6 weeks. The iNICD mice exhibited prolonged sinus bradycardia phenotype one year after cessation of Notch induction.

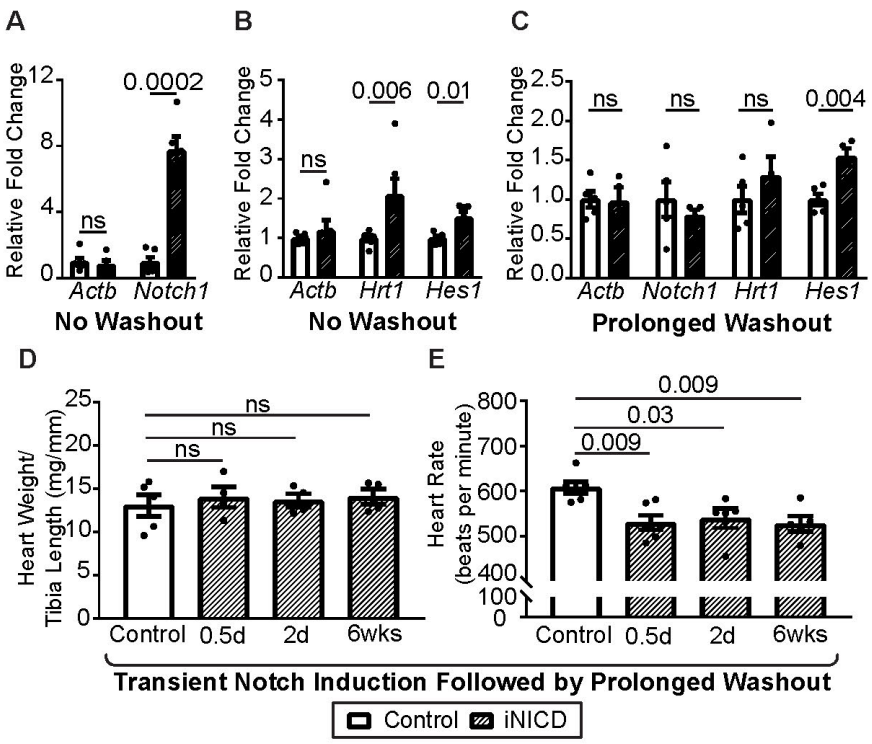

Figure 2.9 Transient Notch activation results in persistent up-regulation of Notch target and prolonged bradycardia. A) N1ICD level in iNICD mice after three weeks of doxycycline chow. B) Up-regulation of direct Notch target genes after 3 weeks of doxycycline chow. C) Persistent up-regulation of Hes1 a year after a 2-day doxycycline induction. D) Ratio of heart weight to tibia length after a one-year washout period. E) Following various induction periods, the iNICD mice demonstrate prolonged sinus bradycardia after a one-year washout period.

2.3.4 Altered expression of key regulators of conduction

Electrical conduction in the heart can be altered by structural and/or molecular changes, such as fibrosis, reduction of gap junctions, and disrupted ion channel expression. Histology and Trichrome staining of the iNICD mice showed healthy atrial myocardium with no signs of fibrosis. The absence of fibrosis in the atria suggests that the slowed atrial CV in iNICD mice may be due to altered cell coupling and reduced excitability as results of electrical remodeling associated with Notch activation. To verify this hypothesis, we performed RT-qPCR on iNICD mice that had undergone the doxycycline induction of two days followed by a one-year washout

to quantify the expression levels of *Cx40*, *Scn5a*, and *Tbx5*. Connexin40 (*Cx40*) is a major gap junction protein in the atrial myocardium and an important regulator of excitation and propagation. Knockout of *Cx40* in mice resulted in conduction slowing and functional block (Bagwe, Berenfeld, Vaidya, Morley, & Jalife, 2005). *Scn5a* encodes for the voltage-gated sodium channel that is responsible for the phase 0 depolarization of membrane potential. Targeted disruption of Scn5a has revealed a direct role of *Nav1.5* channels in SAN conduction and sino-atrial conduction, and suggested an indirect role of the sodium channels in maintenance of the normal SAN pacemaker activity (Lei et al., 2005). *Tbx5*, a critical developmental transcription factor, has previously been shown to regulate the expression of key regulators of conduction including Scn5a in the heart (Arnolds et al., 2012; Nadadur et al., 2016). As shown in Figure 2.9 B, the transient activation of Notch results in significant persistent down-regulation of *Tbx5*, *Scn5a*, and *Cx40* in the right atria. To study the extent of the altered gene expression in the iNICD mice, RNA-sequencing was performed on RA samples from the iNICD mice. The result revealed 888 genes to be differentially expressed, of which the top 25 statistically significant genes are shown to be associated with cardiac arrhythmias. Together with the histological analysis showing a grossly unchanged atrial structure in the iNICD mice, the results suggest that the atrial electrical changes observed from the iNICD mice are likely a direct effect of altered ion channel expression and/or function and not secondary to structural changes.

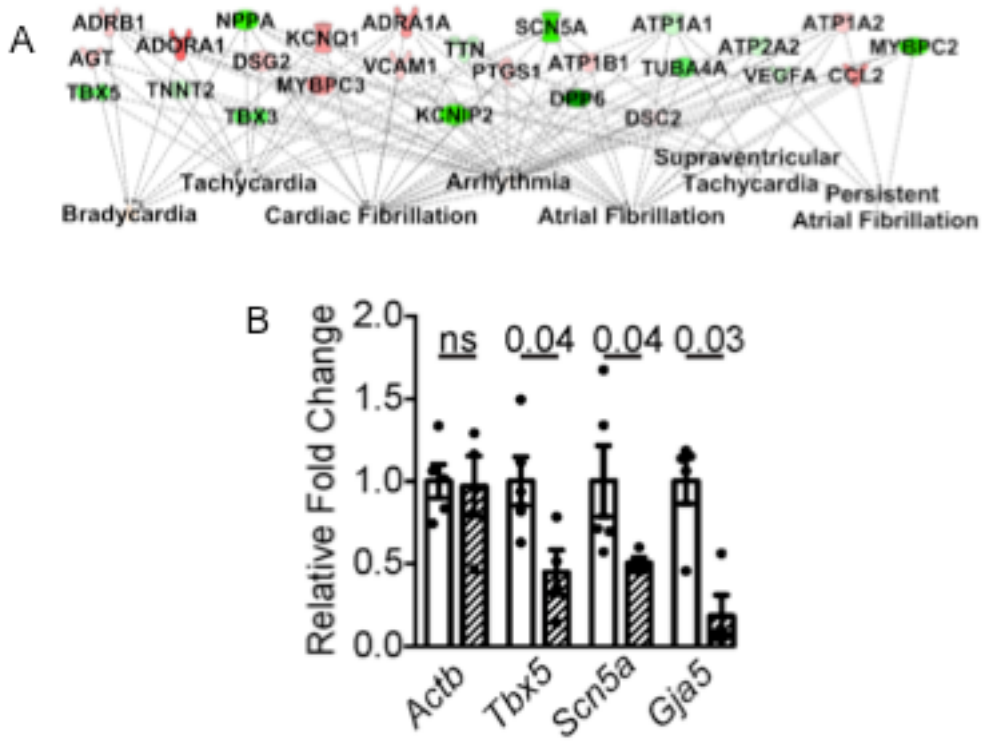

Figure 2.10 Altered expressions of key conduction regulators following transient Notch activation. A) RNA-sequencing of RA from iNICD animals revealed misregulation of genes associated with cardiac arrhythmias. B) RT-qPCR performed on RA samples from iNICD mice showed persistent down-regulation of *Tbx5*, *Scn5a*, and *Gja5*. The iNICD mice undergone the doxycycline induction for two days followed by a one-year washout.

2.3.5 Disrupted conduction following Notch activation predisposes to atrial arrhythmias

Sick sinus syndrome (SSS), also known as sinus node dysfunction, is a group of heart rhythm disorders characterized by sinus bradycardia and sinus pauses, and often is associated with atrial fibrillation (AF) susceptibility. The iNICD mice exhibit sinus bradycardia and sinus pauses, which closely resemble SSS. The reduced CV of in the iNICD RA also results in a reduced critical mass to sustain reentrant arrhythmias. Optical mapping with programmed electrical stimulation near the pulmonary veins was performed to determine if there is an increased susceptibility to AF. The S1S2 programmed stimulation protocol consists of a drive

train followed by a single extrastimulus. As shown in figure The iNICD mice demonstrate significantly greater AF inducibility when compared with the controls as assessed by the percentage of induced AF episodes lasting longer than 1 second (16.7±7.3% vs. 70±18.6%, p = 0.04). To visualize the complex reentrant dynamics of the induced episodes of AF, phase analysis was performed on the optical action potential recorded during AF (Bray, Lin, Aliev, Roth, & Wikswo, 2001; Gutbrod et al., 2015). The analysis revealed stable reentrant circuits mostly anchored around atrial anatomical landmarks with minimal meandering. The center of the reentrant wave was identified by calculating the phase singularity of the phase map using the equation for topological charge. In the example shown in Figure 2.10, the phase singularity overlaps with the inferior vena cava, which acts as the anchor for the anatomical reentry.

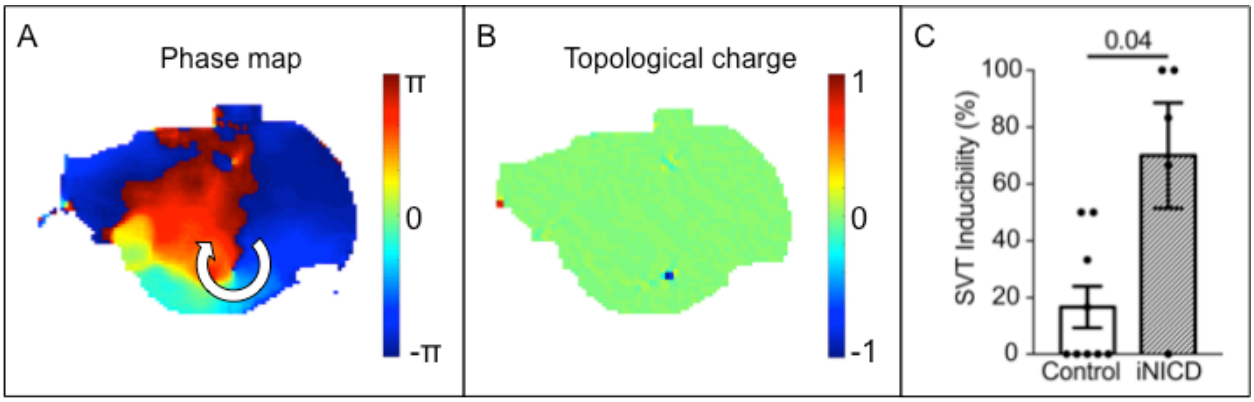

Figure 2.11 iNICD mice exhibited increased SVT inducibility. A) Phase map of an episode of induced reentrant atrial arrhythmia. B) Center of the reentrant wave identified by finding the phase singularity of the phase map using the equation for topological charge. C) The iNICD mice were significantly more susceptible to supraventricular tachycardia (SVT) following S1S2 stimulation.

2.4 Discussion

Here, we have demonstrated that the transient reactivation of Notch in adult mice electrically reprograms the atrial myocardium, resulting in prolonged sinus bradycardia, frequent

sinus pauses, slow heterogeneous conduction, and an increased susceptibility to AF. The phenotype exhibited by our murine model closely resembles SSS. A number of analyses were performed on the telemetry ECG and the optical mapping data to evaluate the sinus bradycardia phenotype. The iNICD mice exhibited preserved diurnal HR response, with slower HR during both periods of high and low activities when compared with the controls. The frequent sinus pauses observed in the iNICD mice had intervals that are not multiples of baseline HR intervals. Optical mapping also revealed 1:1 conduction from the SAN to the distant atrial myocardium. Taken together, these results suggest that impaired response to the autonomic nervous system, intra-atrial block, SAN exit block do not account for the bradycardia observed in iNICD mice. The slowed HR phenotype of the iNICD mice is likely due to slowing of the intrinsic sinus pacemaker rate.

Mutations in genes encoding ion channels or structural proteins have been associated with SSS. Similar to our observation, many of the SSS-associated genes are primarily expressed in the atrial myocardium and not directly in the SAN (Dobrzynski, Boyett, & Anderson, 2007; Mezzano et al., 2016). The qPRC results revealed that Notch activation significantly downregulates *Tbx5*, *Scn5a*, and *Cx40* in the atria. Studies on *Scn5a*$^{+/-}$ mice suggested that disrupted $Na_v1.5$ expression in periphery SAN cells impede their electrical coupling to primary pacemaker cells at the SAN center and result in slowed pacemaker activity (Lei et al., 2005). Numerical modeling has shown that reduction of sodium currents (I_{Na}) in the SAN periphery cells lead to SAN conduction slowing and eventually SAN exit block, which was occasionally observed in the *Scn5a*$^{+/-}$ mice (H. Zhang et al., 2006). In addition, only around 70% of SSS human patients exhibit an abnormal cSNRT (Burnett, Abi-Samra, & Vacek, 1999). The iNICD mice also exhibited no change in cSNRT following programmed stimulation, suggesting there

may be multiple distinct mechanisms causing SSS. A prolonged P wave duration, representing slowed atrial CV, is often a precursor of SSS (De Sisti et al., 1999; Ferrer, 1968) and was also observed in our murine model.

The transient activation of Notch in the adult mice results in transcriptional down-regulation of *Tbx5*, which has been linked with abnormal atrial rhythm and AF susceptibility via the mis-regulation of a number of key regulators of conduction, as shown in figure 2.11 (Nadadur et al., 2016). The reduced Scn5a expression in the iNICD mice results in reduced atrial CV and could cause reduced sodium current and diminished atrial cardiomyocyte excitability. Based on the critical mass theory, the slowed CV in the iNICD atria contribute to a vulnerable substrate for reentrant arrhythmia, evident by the increased SVT susceptibility following programmed stimulation. Taken together, we interpret the increased incidence of pacing-induced SVT together with the paucity of spontaneous atrial arrhythmia episodes during telemetric monitoring of iNICD mice to indicate that although an arrhythmic substrate is present, initiating triggers do not frequently occur in this model.

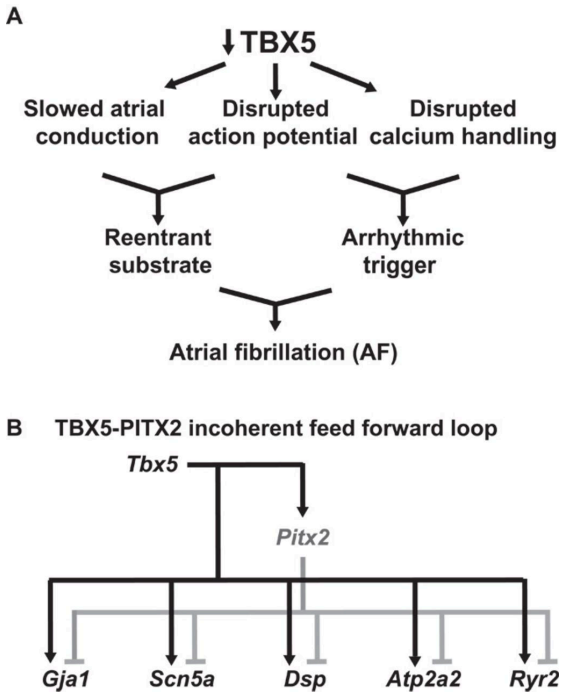

Figure 2.12 *Tbx5* and *Pitx2* interact in a feed forward loop to regulate pacemaking. A) Knockdown of *Tbx5* result in disrupted atrial electrophysiology and AF. B) *Tbx5* and *Pitx2* controls expression of key regulators of conduction in a incoherent feed forward loop (Nadadur et al., 2016).

2.5 Acknowledgement

I would like to acknowledge Catherine Lipovsky, the co-first author on this work, who tirelessly performed most of the molecular work on the project. We would like to acknowledge Carla Weinheimer, Carrie Gierasch, and Attila Kovacs in the Mouse Cardiovascular Phenotyping Core in the Center for Cardiovascular Research for their assistance in performing invasive telemetry studies and echocardiograms, and the Developmental Biology Histology & Microscopy Core at Washington University for assistance with histology. We thank the Genome Technology Access Center in the Department of Genetics at Washington University School of Medicine for help with genomic analysis.

This work was supported by T32 GM007067 (CL), R01 HL130212 (SR), K08 HL107449 (SR), AHA Grant in Aid 14GRNT19510011 (SR), Center for the Investigation of Membrane Excitability Diseases (SR), and Department of Medicine funds from Washington University (SR). Dr. Rentschler holds a Career Award for Medical Scientists from the Burroughs Wellcome Fund.

Chapter 3: Prolonged culture of human cardiac slices and murine atria

Human cardiac slices have emerged as a promising model of the human heart for scientific research and drug testing. Retaining the normal tissue architecture, multiple cell type environment, and the native extracellular matrix, human cardiac slices faithfully replicate the organ-level adult cardiac physiology. In this project, we optimized the organotypic culture condition to maintain normal electrophysiology of the human cardiac slices for 4 days, and demonstrated the capability of cultured isolated murine atrial preparation as a model for studying cardiac pacemaking and exogenous gene expression. The prolonged culture of human cardiac slices and isolated murine atrial preparation demonstrated here enable the *ex vivo* study of chronic drug effects, gene therapies, and gene editing on tissue with organ-level physiology.

3.1 Introduction

Physiologically and genetically accurate models of the human heart are indispensable for studying human cardiac physiology and for pre-clinical screening of candidate biological and drug therapies for their efficacy and/or toxicity. Although crucial for fundamental biological discovery, animal models often fail to predict human response to treatments due to inter-species genetic and physiological differences (Hasenfuss, 1998; Mak, Evaniew, & Ghert, 2014; Nerbonne, Nichols, Schwarz, & Escande, 2001; The FANTOM Consortium and the RIKEN PMI and CLST (dgt), 2014). In recent years, human cardiac slices from donor and end-stage failing hearts have emerged as a promising model of the human heart for electrophysiological and

pharmacological studies (Brandenburger et al., 2012; Camelliti et al., 2011). We have previously demonstrated that human cardiac slices faithfully recapitulate tissue level human cardiac physiology, exhibiting normal conduction velocity (CV), action potential duration (APD), intracellular calcium dynamics, heart rate dependence of these parameters and their response to α- and β-adrenergic stimulation (Kang et al., 2016).

3.1.1 Human cardiac slices exhibit preserved electrophysiology

Optical mapping of human cardiac slices is an intricate process. To record optical action potential with high signal to noise ratio from the slices, every step of the process from tissue collection to dye loading requires optimization (Fig. 3.1). We have previously optimized optical mapping of acutely sectioned slices and have been able to reproducibly record electrical activity from almost all acute slices. When compared with ventricular wedge preparations that can be kept alive for only hours, the major benefit of cardiac slices as a model of human myocardium is its potential ability to test for long-term effect of drugs and exogenous gene modulation. We have invested considerable efforts to improve slice viability in culture and viral transduction efficiency by adapting and improving the culture conditions described in the background section.

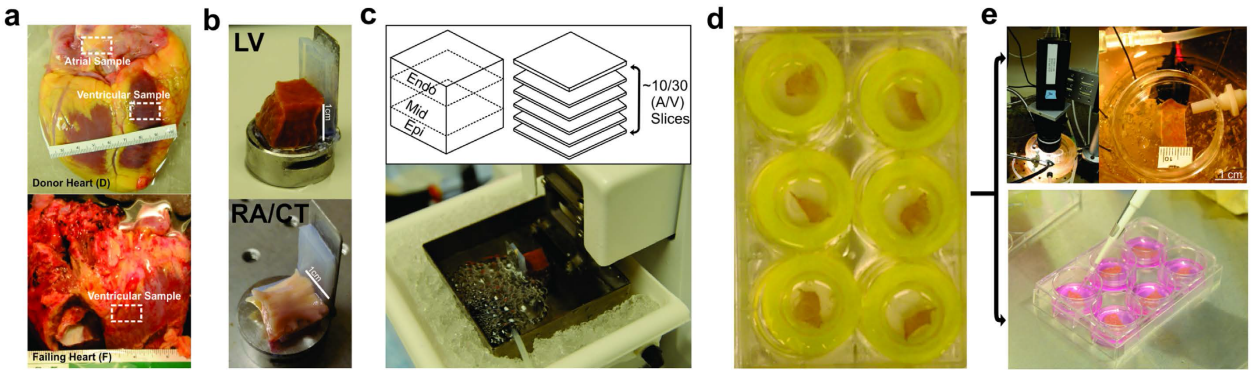

Figure 3.1 Slice preparation pipeline. A) Samples were acquired from atrial and ventricular myocardium of non-failing human donor hearts and end-stage failing hearts. B) The samples were mounted onto a tissue holder with surgical glue. C) A vibratome was used to section the samples into 380μm thick slices

while the tissue is preserved in oxygenated, ice-cold Tyrode's slicing solution. D) The cardiac slices were transferred to Tyrode's washout solution at room temperature to washout BDM. E) After 20 minutes of recovery in the Tyrode's washout solution, the cardiac slices were studied via optical mapping or cultured in 6-well plates (Kang et al., 2016).

To maintain tissue viability in culture, cardiac slices require sufficient oxygen and nutrients. Both factors need to be carefully examined to improve slice viability in culture. In conventional cell culture, oxygen is supplied to the cells via passive diffusion of air across the culture medium. At 380 μm thick, cardiac slices are mostly consisted of myocytes and fibroblasts densely packed in their native three-dimensional extracellular environment, thus may require direct exposure to air for oxygen to sufficiently diffuse across the slices. In the field of neuroscience, Transwell inserts have been widely adopted for the long-term culture of brain slices, since the inserts create a liquid-air interface for greater air diffusion into the tissue (Gahwiler, Capogna, Debanne, McKinney, & Thompson, 1997). To prolong slice viability in culture, we have cultured slices from the same hearts on hydrophilic polytetrafluoroethylene (PTFE) transwell inserts, polyester transwell inserts, and in regular 6-well plates to test the efficacy of different culture conditions. After 24 hours in culture, we were able to electrically stimulate and observe contraction from a significantly greater percentage of slices cultured on PTFE transwell when compared with slices grown in other conditions. Based on this initial observation, the PTFE transwell inserts were used to culture slices for our subsequent work on functional characterization of the slices cultured for 24 hours and for performing viral transduction on the cardiac slices.

Since the culture medium supplies all the necessary nutrients to the slices, the composition of the medium is critical to maintaining slice viability. Three different culture media previously used during culture of cardiac slices or isolated myocytes were compared

(Brandenburger et al., 2012; Habeler, Pouillot, et al., 2009; Habeler, Peschanski, et al., 2009). Since myocytes damage can occur during sectioning of slices which could lead to automaticity, addition of an excitation contraction coupler such as 2,3-butanedione monoxime (BDM) in the medium, which is able to be washed out during subsequent stages, would prevent contraction of the slices and depletion of nutrients in the culture medium. We found that culture medium consisted of M199, 1% penicillin-streptomycin, ITS (Insulin, Transferrin, Selenium) liquid media supplement, and 10 mM BDM.

We have extensively characterized acute human ventricular slices, acute human atrial slices, and ventricular slices that have been cultured for 24 hours. Cardiac slices were obtained from both failing and non-failing donor human hearts. We have been able to optimize the optical mapping procedure to achieve high signal to noise ratio when recording from human cardiac slices (Fig. 3.2A). Since the intensity of the fluorescent signal emitted from the tissue is proportional to tissue thickness, it was difficult to achieve good signal to noise ratio (Efimov et al., 2004; Lang et al., 2011). Extra care is required during the loading of voltage sensitive dye to maintain the health of the tissue and achieve sufficient signal quality. To demonstrate that the cardiac slices are a suitable model for pharmacological assessments, we tested the effect of β - adrenergic stimulation by exposing the slices to 10 nM isoproterenol (Fig. 3.2B). β - Adrenergic stimulation resulted in an expected increase in CV and shortening in APD (Fig. 3.2 D, F). To further compare the cardiac slices with published data on human cardiac tissue, we performed programmed stimulation to measure the APD restitution. The result closely resemble published findings from human ventricular wedge preparations (Fig. 3.2F) (Lang et al., 2015).

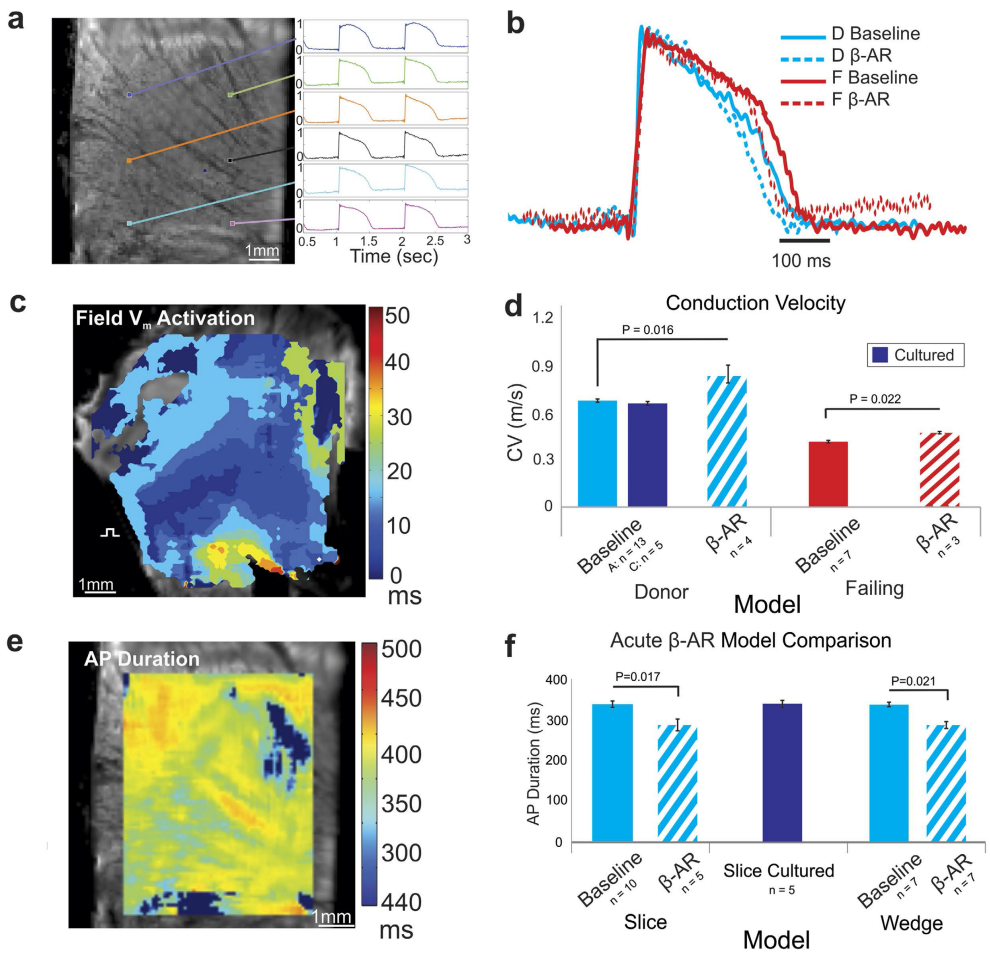

Figure 1.2 Human cardiac slices exhibit normal electrophysiology. A) High signal to noise ratio are achieved when mapping cardiac slices. B) Comparison of AP morphology of failing and non-failing donor slices at baseline and with β-adrenergic stimulation. C) Map of activation sequence of slice under field stimulation. D) Comparison of CVs of acute and cultured donor and failing slices with β-adrenergic stimulation. E) Map of action potential duration 80% at 1 Hz pacing frequency. F) Comparison of APDs of acute and cultured cardiac slices with human ventricular wedge preparation with β-adrenergic stimulation (Kang et al., 2016).

The human cardiac slices also demonstrate physiological CV, similar to what have been reported in human ventricular wedge preparations (Lang et al., 2015). As shown in figure 3.2 D, ventricular slices cultured for 24 hours maintained its normal CV under baseline condition. The acute and cultured ventricular slices exhibit normal APD and CV characterizes similar to what have been reported in perfused human ventricular wedge preparations (Lang et al., 2015). These

data demonstrated our ability to maintain electrophysiology of the ventricular slices for 24 hours in culture.

Due to the limited supply of fully intact human atria, studying human atrial electrophysiology using perfused atrial preparation is extremely challenging. It is also difficult and impractical to maintain perfusion-based tissue preparations for long term studies of chronic drug exposure or gene therapy. We have been able to obtain human atrial slices with electrophysiology similar to what have been reported from perfused human atrial preparations (Fig. 3.3) (Fedorov et al., 2011). The atrial slices are obtained from the crista terminalis (CT) because of the difficulties in obtaining intact slices from the highly trabeculated atrial free wall. Optical mapping revealed the presence of pacemaker cells in the atrial slices, as demonstrated by the difference in the morphologies of calcium (Ca^{2+}) transients (Fig. 3.3 B and C). The Ca^{2+} transient recorded from atrial myocardium exhibits fast upstroke and recovery, while the Ca^{2+} transient from the SAN has slow upstroke and prolonged recovery period. Some of the atrial slices also demonstrated automaticity. Extra beats can be observed at lower pacing rates (Fig. 3.3 E). Without electrical stimulation, some of the atrial slices collected from the CT exhibit automaticity at approximately 1Hz.

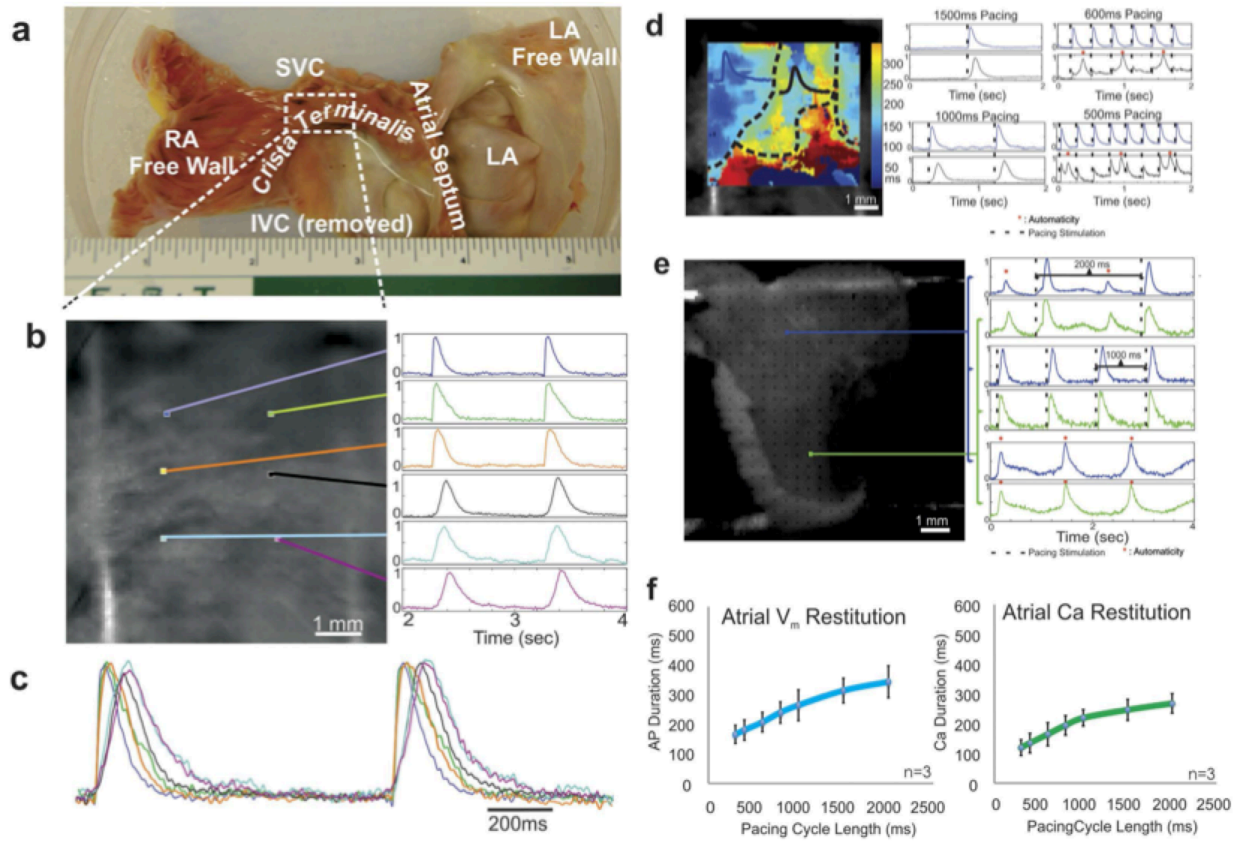

Figure 3.3 Electrophysiology of acute human atrial slices. A) Atrial slices are obtained from crista terminalis. B) High signal to noise ratio can be obtained when mapping Calcium (Ca^{2+}) transient on atrial slices. C) Heterogeneity can be observed in the Ca^{2+} morphology. Faster Ca upstroke and recovery corresponds to atrial working myocytes. Slow Ca^{2+} upstroke and recovery corresponds to SAN cells. D) At 1Hz pacing, both cell types are fully captured. However, the SNA cells fails to capture at higher pacing rates. E) Optical mapping of AP revealed automaticity in the atrial slices. F) Restitution curves of AP and Ca^{2+} in atrial myocytes are significantly lower than those of ventricular slices (Kang et al., 2016).

Translating our knowledge of viral transduction on murine atria to the human cardiac slices, we were able to transduce the slices with adenovirus encoding for eGFP (Ad5-GFP) and observe eGFP expression 2 days after transduction. However, the combination of trypsin and collagenase resulted in significant loss of tissue integrity in the slices. To preserve tissue integrity while maximize viral transduction efficiency, we tested a number of conditions and found that treating the slices with virus-collagenase mixture for only for 10 minutes produced the best outcome. As shown in Figure 3.4, the virally transduced cardiac slices exhibited strong

expression of the virally-encoded eGFP for 96 hours. The expression of the exogenous gene in cardiomyocytes was verified by co-staining the tissue with a myocyte specific marker α-Actinin. To examine the degree of tissue remodeling during culture, immunohistochemical staining of Connexin 43 (Cx43), the major gap junction protein in the ventricles, was performed on the virally transduced slices. As shown in figure 3.4, the expression of Cx43 at the intercalated discs was largely preserved for 96 hours.

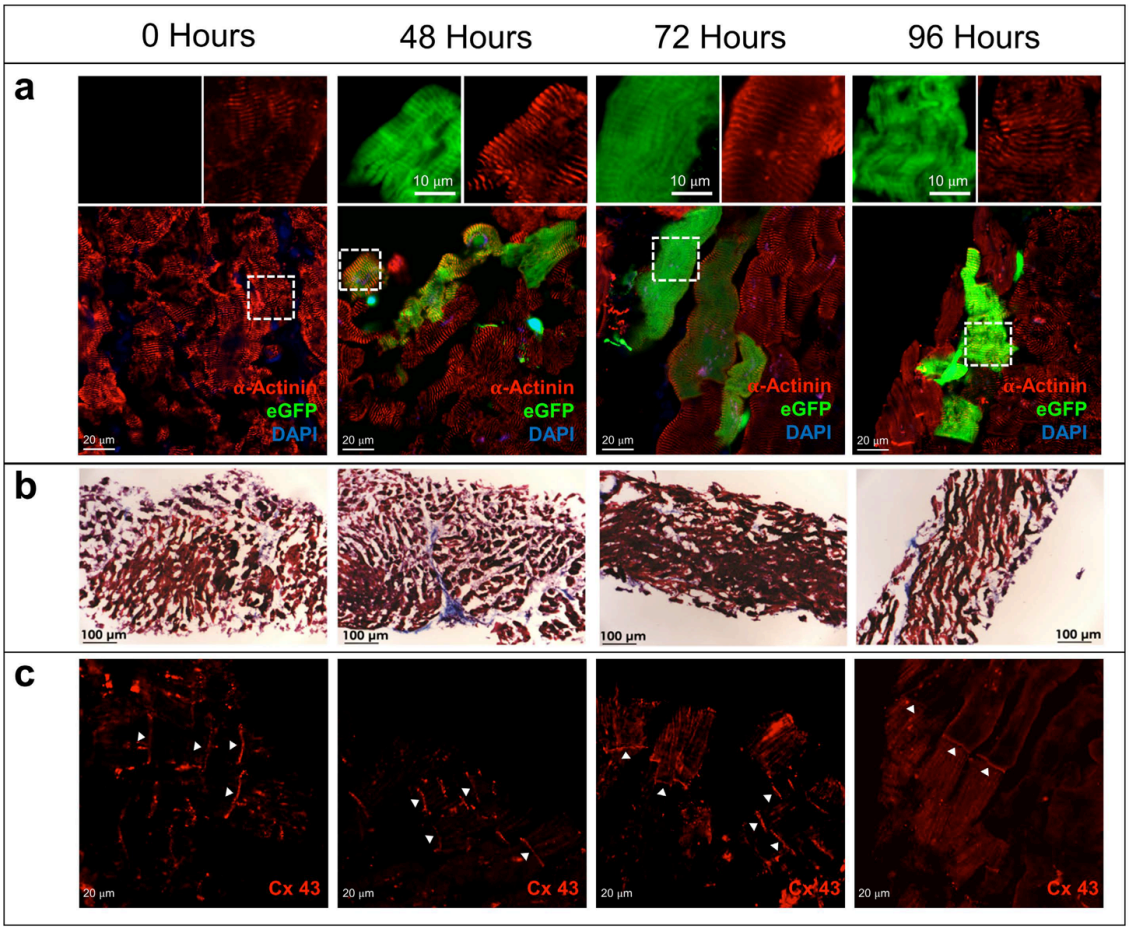

Figure 3.4 Viral transduction of human cardiac slices with adenovirus. A) Expression of eGFP after viral transduction with Ad5-eGFP. The merged images show eGFP (green), α-Actinin (red), and nuclei DAPI staining (blue). B) Masson's trichrome stain shows preserved structure of the ventricular cardiac slices. C) Immunohistochemical examination of Cx43 in the cardiac slices shows preserved gap junction expression (Kang et al., 2016).

3.1.2 Isolated murine atria as a platform for studying cardiac pacemaking and transcriptional reprogramming of the atrial myocardium

The rhythmic contraction of the heart is initiated and maintained by the spontaneous firing of the SAN pacemaker cells. The spontaneous activity of the SAN cells are triggered by a slow diastolic depolarization till the membrane potential reaches the threshold of T-type and L-type Ca2+ channel activation1. The diastolic depolarization of SAN cells is mainly due to the activation of the funny current (I_f), which is governed by the hyperpolarization and cyclic nucleotide (HCN) channel2. In addition to the voltage clock, SAN cells also require a Ca^{2+} clock that maintains the spontaneous Ca^{2+} release from the sarcoplasmic reticulum3. Failure of the SAN to generate electrical impulses is common and can have severe consequences. The isolated murine atria have been extensively studied as a platform for studying cardiac pacemaking (Di paper). The organotypic culture of the murine atria would enable the use of the tissue for studying the effect of transcriptional reprogramming *ex vivo*. The native tissue environment preserved in the atria culture maintains the normal extracellular matrix and allows for intercellular communication, which is crucial for the differentiation and maintenance of native morphology of cardiomyocytes.

3.2 Methods

3.2.1 Collection of human heart

Experimental protocols were approved by the George Washington University Institutional Review Board and were in accordance with human research guidelines. Human donor hearts rejected for organ transplantation were procured from Washington Regional

Transplant Service (Washington, DC). Consents were obtained either from donors as previously granted or from family members allowing use of the hearts for research purpose. Following aortic cross-clamp, the hearts were cardioplegically arrested using University of Wisconsin (UW) solution (ViaSpan) in the operating room. The hearts were transported in the UW solution on ice.

3.2.2 Slice preparation

The procedures for slice preparation and culturing were described previously in detail (Kang et al., 2016). A sample approximately 1cm x 1cm x 1cm was cut from the left ventricular (LV) free wall. Care must be taken to ensure that the tissue is submerged in solutions at all times. The tissue samples were mounted onto the tissue holder of a vibrating microtome (Campden Instruments, UK) and sectioned into 380 μm thick slices while submerged in a modified Tyrode's solution (140mM NaCl, 6mM KCl, 10mM Glucose, 10mM Hepes, 1mM $MgCl_2$, 1.8mM $CaCl_2$, 10mM BDM, pH 7.4). The cutting chamber was surrounded by ice to maintain a stable low temperature. The vibrating microtome was set to 0.4 mm/s advance speed, 2 mm horizontal vibration amplitude at 80 Hz. Importantly, to minimize trauma to the tissue during sectioning, the undesired vertical vibration of the blade was laser-calibrated to less than 0.5 μm. After sectioning, each slice was placed in a cell straining and weight down with a meshed ring and transferred to a bath of modified Tyrode's washout solution (140mM NaCl, 4.5mM KCl, 10mM Glucose, 10mM Hepes, 1mM $MgCl_2$, 1.8mM $CaCl_2$, pH 7.4). The slices were kept in the washout solution for 20 minutes before optical mapping or culturing to washout BDM and reduce temperature shock.

3.2.3 Culture of human cardiac slices in a tri-gas incubator

To prevent contamination, the cardiac slices were rinsed three times in sterile phosphate buffered saline (PBS) before culturing. The forceps used to handle the slices were sterilized with a bead sterilizer between each rinse. The slice culture medium consisted of Medium 199 (M4530, Sigma-Aldrich, St. Louis, MO), 1 x ITS (I3146, Sigma-Aldrich, St. Louis, MO), and 2% penicillin streptomycin (P4333, Sigma-Aldrich, St. Louis, MO). The slices were cultured in 6-well plates with one slice in each well and 3 mL of the culture medium. To facilitate oxygen diffusion into the slices, the plates were agitated on an orbital shaker at 20 rpm placed inside a tri-gas incubator (Thermo Fisher Scientific, Waltham, MA) with 30% O_2 and 5% CO_2 at 37°C. The culture medium was changed every two days.

3.2.4 Optical mapping of human cardiac slices

A CMOS camera imaging system (ULTIMA-L, SciMedia, Costa Mesa, CA) was used to measure changes in transmembrane potential in the acutely isolated and cultured murine atria and human slices. Both types of tissue were superfused in Tyrode's washout solution at 37°C with the pH maintained at 7.4. To eliminate motion artifacts in the recorded optical signal, the isolated atrial tissue was immobilized using the excitation-contraction uncoupling agent, blebbistatin (10μM), which has been shown to have no significant effects in action potential (AP) morphology. Subsequently, the tissue was stained via superfusion with a voltage-sensitive dye, Di-4-ANEPPS (61010, Biotium, Fremont, CA). A green LED light source (Prizmatix, Southfield, MI) with the wavelengths of 520±45 nm was used to excite the voltage-sensitive dye.

The emitted fluorescence was filtered by a long-pass filter at 650 nm and collected by the ULTIMA-L camera as previously descried (Kang et al., 2016).

3.2.5 Optical mapping data analysis

The recorded data was first visualized using Brainvision software and then analyzed using Rhythm, our open source custom developed MATLAB program (Laughner, Ng, Sulkin, Arthur, & Efimov, 2012). The optical action potential signal was filtered with a 100Hz low-pass filter, 3x3 binning, and a 1st order drift correction. Activation maps of the isolated atrial tissues were generated based on the maximum derivatives of the optical signals (dVm/dt_{max}). Activation maps of the human tissue paced at a cycle length of 1000 ms were used to calculate the conduction velocity. Action potential duration was calculated by measuring the time elapsed between depolarization and 80% repolarization.

3.2.6 Viral transduction on cardiac slices

To maximize viral transduction efficiency, 5 uL of type 2 collagenase (375 units/mL) are mixed with 2uL of adenovirus expressing green fluorescent protein (Ad5-GFP) (10^12 v.p/mL) and added to a cardiac slice. After incubating for 10 minutes, the tissue is washed with DMEM with 10% FBS and PBS. The slice culture medium is added to each well before the plate is placed back into the incubator.

3.2.7 Dissection of murine atria

Mice were anesthetized with Ketamine and injected with heparin in accordance with approved animal protocol. After loss of withdraw reflex, thoracotomy will be performed to excise the heart. The excised heart will be placed in oxygenated Tyrode's solution with pH equilibrated to 7.4 at 37°C. With the posterior side of the heart facing up, a cut will be made slightly above the midsection of the heart to remove the ventricles. Facing the same orientation, an incision from the tricuspid valve to the superior vena cava along the atrial septum will be made under a surgical microscope. Subsequently, portions of the atrial septum will be removed to open the left atria. The edges of the atria will be slightly stretched and pinned to expose the endocardial surface. The resulting isolated atria preparation will contain the intact SAN region, delimited by the crista terminalis, atrial septum, and orifice of the superior vena cava.

3.2.8 Culturing of murine atria

To culture the isolated murine atria, the tissue will be sterilized by rinsing in sterilized phosphate buffered saline (PBS) for multiple times. The sterilized tissue will be immediately transferred to six-well dishes coated with silicon. The edges of the isolated atria will be slightly stretched and pinned to the bottom of each well. The basic culture media will be consisted of Medium 199, 10% Fetal Bovine Serum (FBS), and 1% penicillin streptomycin (PS). The isolated atria will be cultured in a tissue culture incubator with constant humidity at 37°C and at 5% CO_2. To promote superfusion of the media, the six-well dishes containing the atrial tissue will be placed on top of an adjustable speed orbital shaker set at 20 rpm. The culture media will be changed daily to reduce the chance of contamination.

3.2.9 Gene painting on isolated murine atrial preparation

The isolated murine atria preparations will be painted immediately after the tissue is pinned in the culturing plate. A gel mixture will be made with 20% poloxamer and 0.5% trypsin in PBS. Recombinant adenovirus expressing plasmid for the genes of interest will be added to the mixture for a final viral titer of at least 1 x 10^{11} virus particles per mL. The mixture is liquid in consistency at 4°C, but gels at room temperature. Using a soft fine painter's brush, 5 µL of the gel mixture containing the adenovirus will be applied directly to specific regions of the isolated atria.

3.3 Results

With preserved extracellular matrix and native cell-cell coupling, vibratome-cut human cardiac slices have been demonstrated as an authentic model of the adult human heart for physiological studies and pharmacological testing (Brandenburger et al., 2012; Camelliti et al., 2011; Kang et al., 2016). We have previously established a protocol for obtaining viable human cardiac slices from non-failing donor hearts that were rejected for transplantation and from end-stage failing hearts (Kang et al., 2016). In this project, we further optimized the culture condition to extend viability length of the cardiac slices *in vitro*. Using optical mapping, we evaluated the conduction parameters of the culture cardiac slices.

3.3.1 Long-term culture of human cardiac slices

Extending the culture length of the cardiac slices while preserving the mature phenotype would enable the study of human cardiac physiology and the test of chronic pharmacological perturbation and gene therapies. Without microvasculature perfusion, the cardiac slices rely entirely on passive diffusion of oxygen and nutrients. At 380µm, the thickness of the slices

approaches the diffusion limit of oxygen in soft tissue (Barclay, 2005). We previously cultured the cardiac slices on a liquid air interface to facilitate oxygenation of the slices and were able to preserve normal electrophysiology for 24 hours (Kang et al., 2016). In this project, we modified the culture protocol to increase oxygenation of the liquid culture medium. A tri-gas incubator with 30% O_2, 5% CO_2 at 37°C was used to culture the slices. The slices were individually cultured in 6 well plates with 3mL of medium in each well. The culture plates were placed on an orbital shaker set at 20 rpm to further increase the dissolved oxygen concentration in the liquid culture medium (Fig 3.5).

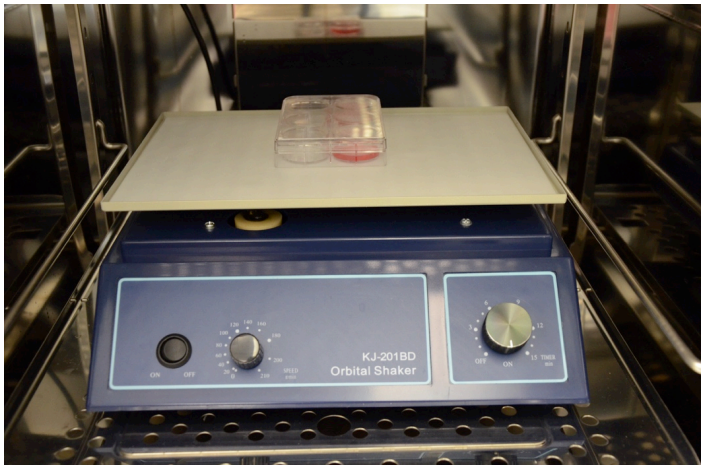

Figure 3.5 Setup for culturing human cardiac slice in a tri-gas incubator.

Human cardiac slices obtained from the left ventricular free wall remained electrically viable for up to 21 days *in vitro* and routinely maintained normal electrophysiology for up to 4 days, as shown in Figure 3.6. We performed optical mapping to measure the conduction parameters of the cardiac slices. The conduction velocity was measured at 1 Hz pacing. When compared with fresh slices, the cultured slices maintained anisotropic conduction (Fig. 3.6 D), and uniform repolarization across the entire slice (Fig. 3.6 F). The slices demonstrated preserved physiological conduction velocity for 4 days in culture (Day 0: 21.3±4.5 cm/s, Day 2:

19.7±1.8cm/s, Day 4: 17.2±1.7cm/s, Day 0 vs. Day 2: p = 0.76, Day 0 vs. Day 4: p = 0.14), as shown in Figure 1A. However, significant reduction in CV was observed in the slices cultured for 21 days (6.7 cm/s). The slowed conduction in the long-term slice culture may be a manifestation of tissue remodeling and dedifferentiation due to the lack of electrical and mechanical loading.

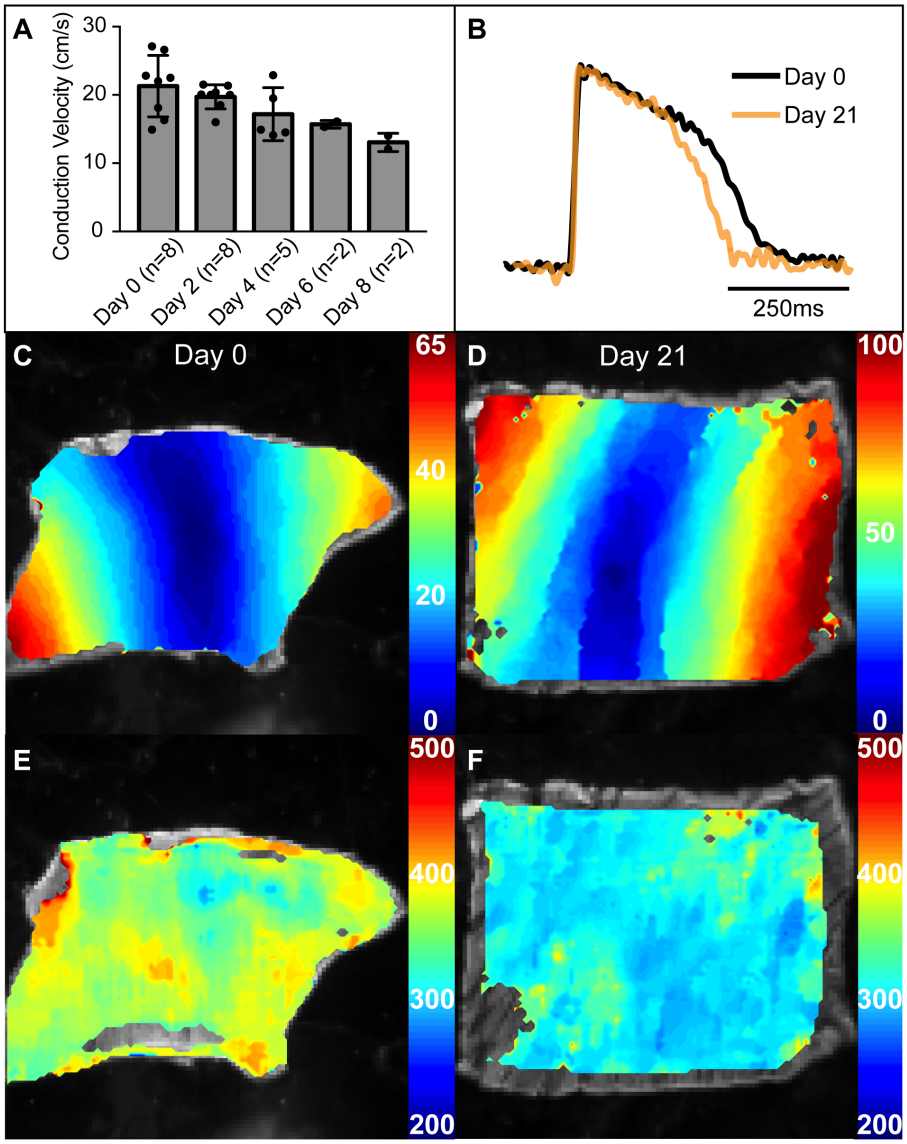

Figure 3.6 Cultured human cardiac slice electrophysiology. A) CV of cultured human cardiac slices overtime. No significant changes in conduction velocity were observed in slices cultured for 2 days and 4 days when compared with fresh slices. B) Comparison of action potentials of a fresh human cardiac slice

and a slice cultured for 21 days. C) Activation map of the fresh slice. The colorbars represent activation times in ms. D) Activation map of the cardiac slice cultured for 21 days. E) APD map of the slice shown in panel C. F) APD map of the slice shown in panel D.

3.3.2 Long-term culture of isolated murine atrial preparation

As a platform for testing varies reprogramming strategies, organotypic culture of isolated adult murine atria has been developed. Organotypic culture of the atria has unique advantages over isolated cardiomyocytes culture. The native tissue environment preserved in the atria culture maintains the normal extracellular matrix and allows for intercellular communication, which is crucial for the differentiation and maintenance of native morphology of cardiomyocytes. Organotypic culture is well established and widely used in the study of brain, kidney, liver, lung, and pancreas in the form of tissue slices (Parrish, Gandolfi, & Brendel, 1995). Our results (Fig. 3.7) are the first to demonstrate the feasibility of culturing electrically viable isolated adult murine atria for extended period of time. After 5 days in culture, the isolated atria demonstrated stable HR, physiological atrial CV, and stable pacemaker site within the SAN area.

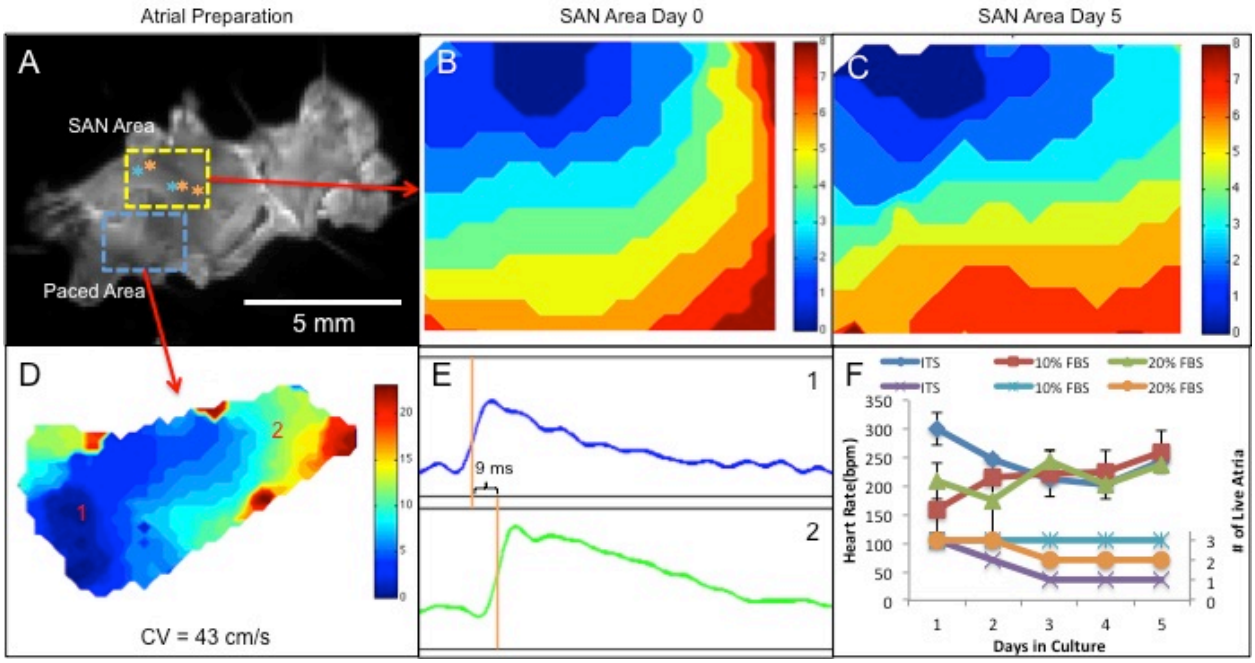

Figure 3.7 Culture of isolated murine atrial preparation. A) Photograph of the adult murine atrial isolation. B-C) Maps of activation recorded optically on day 0 and day 5 of culture near the SAN. The activation time is shown in ms. D) Map of activation during pacing. E) Representative optical action potentials from sites 1 and 2 shown in panel D. F) Stability of heart rate when cultured with different media.

To obtain the tissue preparation, atria was removed from a Langendorff-perfused heart and dissected open, as shown in Figure 3.7 A. The isolated atria were cultured in 6-well plates coated with polydimethylsiloxane (PDMS) for anchoring the tissue with micro dissection pins. The first sites of atrial activation in acutely isolated atria are represented by the blue dots in Figure 3.7 A; whereas the orange dots are the first sites of activation in the cultured atria. The location of the pacemaker site remained stable in the cultured atria when compared with the acute conditions. As shown in Figure 3.7 B and C, the pacemaker sites of the acutely isolated and cultured atria remained in the anatomically defined SAN region, and the normal activation pattern was preserved. A magnified activation map of cultured atria that was paced at a cycle length of 100 ms is shown in Figure 3.7 D. The conduction velocity of the cultured atrial tissue was within the normal physiological range, and it was calculated by taking the distance and

activation times at location 1 and 2. The optical signals at the two locations and the difference in their activation times are illustrated in Figure 3.7 E. As shown in Figure 3.7 F, murine atria cultured in the medium supplemented with 10% FBS maintained the highest viability (ITS: Medium 199 (M199), 1% ITS Liquid Media Supplement, 1% penicillin-streptomycin (PS); 10% FBS: M199, 10% Fetal Bovine Serum (FBS), 1% PS; 20% FBS: M199, 20% FBS, 1% PS). Far-field electrocardiography was performed daily on the cultured atria. The sinus rhythm of the isolated atria remained stable throughout the duration of the culture. These results show that isolated murine atria can be consistently cultured for an extended period of time while maintaining their normal electrophysiology.

Isolated and cultured murine atria are a useful platform for optimizing viral transduction. When compared with viral transduction in cell culture, achieving high transduction efficiency is much more difficult when working with *ex vivo* tissue due to the dense extracellular matrix. We adapted a localized gene delivery technique called "gene painting" to deliver adenovirus to murine atria (Kikuchi, McDonald, Sasano, & Donahue, 2005; Swaminathan et al., 2011). Proteases such as trypsin and collagenase were mixed with the virus to digested part of the extracellular matrix to allow transmural penetration of the virus into the tissue. Adenovirus expressing green fluorescent protein (Ad5-GFP) is used since the resulting eGFP expression would be an easy readout for transduction efficiency. As shown in Figure 3.8, gene painting of the cultured murine atria with Ad5-eGFP resulted in localized eGFP expression 2 days after the viral transduction.

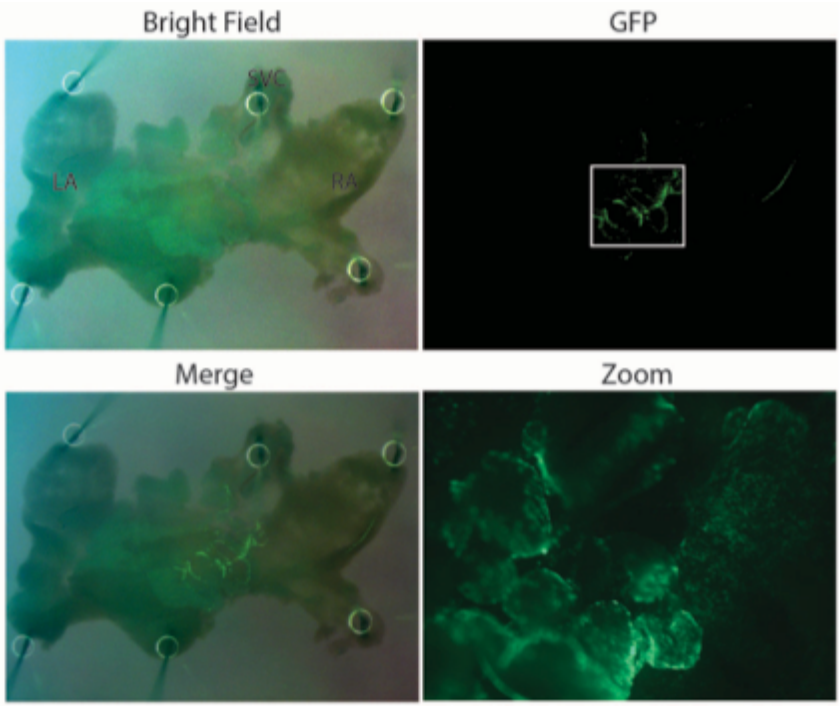

Figure 3.8 Viral transduction of cultured mouse atrial preparation with gene painting.

3.4 Discussion

We have previously demonstrated the advantages of human cardiac slices as a model for studying human cardiac physiology and for drug efficacy and toxicity testing (Kang et al., 2016). However, the limited culture duration and the intricate culture protocol impeded the use of human cardiac slices for long-term studies. Here, we present an improved culturing method that maintains normal electrophysiology of the human cardiac slices for 4 days, which enables research of chronic drug exposure and exogenous gene expression.

Several studies have demonstrated the feasibility of maintaining cardiac slice viability in culture, but have observed significant tissue remodeling in the slices cultured long term. In the absence of electrical and/or mechanical stimulations, cardiomyocytes undergo significant remodeling and dedifferentiation, evident by diminished contractile force, triangulation of action

potential morphology, and reduced gap junction expression(Brandenburger et al., 2012; Kaneko et al., 2012). We demonstrated that the cultured human cardiac slices maintain normal electrophysiology for up to 4 days and remain electrically viable for up to 21 days when cultured inside a high oxygen environment. Significant reduction in CV was observed in the cardiac slices cultured longer than 4 days. The reduction in CV of the cultured slice is likely due to tissue dedifferentiation in the absence of electrical and mechanical stimulation. To overcome this, we subsequently developed a culture system with electrical stimulation and mechanical anchoring capabilities as a platform to optimize organotypic culture of the human cardiac slices.

We utilized optical mapping to characterize the conduction parameters of the cardiac slices at a high spatial and temporal resolution. Optical mapping is also capable of measuring other functional parameters such as the intracellular calcium and the metabolic state, using calcium-sensitive fluorescent dyes and NADH fluorescence (Lou, Li, & Efimov, 2011; Moreno, Kuzmiak-Glancy, Jaimes, & Kay, 2017). However, the use of fluorescent probes in optical mapping hampers its ability to take repeated measurements on the same slice over the length of culture. To overcome this, other techniques such as intracellular microelectrode recording and multi-electrode array recording can be applied to study the cardiac slices (Camelliti et al., 2011). The prolonged culture of human cardiac slices demonstrated here enables the study of chronic drug effects, gene therapies, and gene editing. Adenoviral (Ad) vectors are a promising approach for *in vivo* gene delivery because the ease of producing high titer when compared with lentivirus and the larger packaging capacity when compared with adeno-associated virus (Thomas, Ehrhardt, & Kay, 2003). However, the clinical adoption of Ad vectors for gene therapy has been limited by its dependence on the coxsackievirus and adenovirus receptor (CAR) for transduction (Dmitriev et al., 1998). With the preserved native extracellular matrix, the cardiac slices are a

powerful platform for testing advancements in vector technology, such as tropism-modified CAR-independent Ad5 vectors.

With the prolonged culture length, human cardiac slices can be used as an accurate model of the human myocardium for testing the effect of exogenous gene expression. Optogenetic stimulation and inhibition with light-gated ion channels such as Channelrhodopsin-2 (ChR2) and anion channel rhodopsins (ACRs) has been proposed as a selective and safe method of cardiac pacing and cardioversion (Govorunova, Sineshchekov, Janz, Liu, & Spudich, 2015; Jia et al., 2011). With built-in LED light source and far field-sensing electrodes, our culture system can perform automated evaluations of optogenetic stimulation on specific regions of the adult human heart. RNA interference (RNAi) has been proposed as a potential therapeutic and research tool. The ability to silence specific genes of interest with small interfering RNA (siRNA) and short hairpin RNA (shRNA) makes RNAi a powerful tool for studying cardiac physiology (Poller, Hajjar, Schultheiss, & Fechner, 2010; Suckau et al., 2009). The approach has been used for suppressing inflammatory response and oxidative stress to improve cardiac function following myocardial infarction in animal models (Hong et al., 2014; Somasuntharam et al., 2013). When applied to human cardiac slices, RNAi can be used to gain valuable insights to human cardiac physiology by selective knockdown of specific ion channels and subunits.

With preserved SAN function and anatomical structures, the isolated murine atrial preparation is an accurate platform of the atria for studying cardiac pacemaking and for developing transcriptional reprogramming protocols for the generation of biological pacemakers (Choate & Feldman, 2003; Schmidt & Nygren, 2006). Most commonly due to age-related degeneration, SSS exhibits symptoms such as irregular prolonged pauses between heartbeats, pathologically slow resting HR, and inadequate activity-related increase in HR (Ferrer, 1968).

Currently, transvenous implantation of permanent electronic pacemakers is the only effective treatment for patients with SAN dysfunction. Pacemaker therapy using implantable electronic devices has a number of significant limitations. Major risks associated with electronic pacemakers include infection at the surgical site, limited battery life, lack of activity-related modulation of HR, and device or electrodes failure (Kiviniemi, Pirnes, Eränen, Kettunen, & Hartikainen, 1999). Unique issues may arise in pacemaker therapy for pediatric patients such as lead migration due to heart development. Due to these complications and malfunctions, majority of patients with pacemakers require reoperation (Fleck, Khazen, Wolner, & Grabenwoger, 2006).

The need for a smarter and more reliable pacemaker has driven the biological pacemaker research, with the goal of generating a permanent and autonomically sensitive pacemaker using cell-based approaches or viral-based gene therapy. To create a functional biological pacemaker, the engineered cells not only need to have appropriate gene expressions and functional behavior, but also need to exhibit correct three-dimensional anatomical and molecular architecture to allow for source-sink matching. One approach is to differentiate pluripotent stem cells into pacemaker cells *in vitro* by recapitulating normal developmental programs, followed by direct injection of cells into the heart (Kehat et al., 2004). However, it would be difficult to produce a highly functional pacemaker since the 3D anatomical structure of the biological pacemaker cannot be effectively controlled due to low cell retention and engraftment after myocardial injection. Atria would also be a more ideal location to generate a biological pacemaker to treat SAN dysfunction. Another approach is to directly reprogram adult atrial cardiomyocytes to pacemaker cells in situ using viral-based delivery of transcription factors (Kapoor, Liang, Marbán, & Cho, 2013; Miake, Marbán, & Nuss, 2002). Reactivation of developmental programs in adult tissue to promote tissue regeneration during injury responses has been well studied. Terminally differentiated cells

are currently being directly converted into a new cell type of interest for therapeutic benefits via reactivation of developmental programs (Hanna et al., 2008). The benefit of the transcriptional reprogramming approach is that maintenance of gene expression will not be required for phenotypic maintenance once cellular reprogramming has occurred. It has been demonstrated that reprogramming of murine ventricular cardiomyocytes into specialized conducting Purkinje-like cells via activation of the Notch signaling pathway, which is a developmental signaling cascade that regulates specification of the conduction system (Rentschler et al., 2012). Using a similar approach, *Tbx18* has been recently demonstrated to reprogram adult guinea pig ventricular cardiomyocytes into induced-SAN cells (Kapoor et al., 2013). However, the reprogramming effect of *Tbx18* was not tested in the atrium, which is the ideal location for a biological pacemaker to approximate normal physiology. In addition to *Tbx18*, several other transcription factors have also been demonstrated to be involved in the development of the SAN, including *Tbx3*, *Shox2*, and canonical *Wnt* signaling (Bressan, Liu, & Mikawa, 2013; Liu et al., 2012; Wiese et al., 2009). In this project, we have developed a robust protocol for organotypic culturing of adult murine atria and explored a targeted gene delivery technique for spatial specific genetic manipulation. The organotypic culture of isolated murine atrial preparation enables efficient screening of various transcription factors for their effects in direct reprogramming of mature working atrial myocardium into a biological pacemaker.

3.5 Acknowledgement

I would like to give special acknowledgement to Dr. Chaoyi Kang, who pioneered the use of optical mapping technique for electrical characterization of human cardiac slices. I would also like to acknowledge Rich Li, for his instrumental help with viral transduction of the cardiac

slices. We are grateful to Mid-America Transplant Services for kindly providing us with the human cardiac tissue. We thank Dr. David Curiel for providing us with the adenovirus for the project. We are also grateful to all members of the Efimov lab and the Rentschler lab for critical discussion of the project.

Chapter 4: Novel platform for the investigation of normal and pathological human cardiac physiology

Human cardiac slices have emerged as a promising model of the human heart for scientific research and drug testing. Retaining the normal tissue architecture, multiple cell type environment, and the native extracellular matrix, human cardiac slices faithfully replicate the organ-level adult cardiac physiology. In this project, we optimized the organotypic culture condition to maintain normal electrophysiology of the human cardiac slices for 4 days and developed an automated, self-contained heart-on-a-chip system for maintaining tissue viability and for transporting live tissue. The prolonged culture of human cardiac slices demonstrated here enables the study of chronic drug effects, gene therapies, and gene editing. To achieve long-term culture and to minimize tissue dedifferentiation, the culture system supports media circulation, oxygenation, temperature control, electrical stimulation, and mechanical loading. The culture parameters can be individually adjusted to establish the optimal culture condition. The development of the heart-on-a-chip technology presented here further facilitate the use of organotypic human cardiac slices as a platform for pre-clinical drug testing and research in human cardiac physiology.

4.1 Introduction

Extensive efforts have been invested into developing an authentic model of the human heart. Human induced pluripotent stem cell derived cardiomyocytes (hiPSC-CMs) are widely used in modeling diseases and drug screening (Chi, 2013; Itzhaki et al., 2011). However, the

development of hiPSC-CMs with mature atrial or ventricular phenotype has been challenging so far (Karakikes, Ameen, Termglinchan, & Wu, 2015; Robertson, Tran, & George, 2013). Another approach to study human cardiac cell biology involved isolated primary human cardiomyocytes, which are functionally mature, but have limited experimental duration since they dedifferentiate in cell culture (Bird et al., 2003; Coppini et al., 2014). Different cardiomyocyte subpopulations can be obtained by altering the cell isolation process. However, they exhibit altered electrophysiology, i.e. action potential morphology, due to the lack of cell-cell coupling and membrane protein alterations caused by the tissue digestion procedure. The cell isolation procedure is also time consuming and labor intensive, thus limiting the use of isolated cardiomyocytes to low-throughput testing. Another approach is based on the human ventricular wedge preparations, which allow for studying CV, conduction heterogeneity, and arrhythmia susceptibility (Glukhov et al., 2012; Glukhov, Fedorov, et al., 2010; Lou, Fedorov, et al., 2011). Due to the complexity and variability of the coronary system and the size constraint of the preparation, the ventricular wedge preparation is also severely limited in terms of throughput. Primary cells, cell lines, and tissue also have significantly different gene expression profiles, as reported by the functional annotation of the mammalian genome 5 consortium (The FANTOM Consortium and the RIKEN PMI and CLST (dgt), 2014). Human cardiac slices faithfully replicate the organ-level adult cardiac physiology because they retain the normal tissue architecture, multiple cell type environment, extracellular matrix, etc (Kang et al., 2016). At the diffusion limit for oxygen, human cardiac slices can be cultured long-term for studying chronic drug treatment, gene expression regulation, and genetic engineering (Barclay, 2005; Brandenburger et al., 2012; Bussek et al., 2012; Kang et al., 2016).

Previous studies on the organotypic culture of ventricular slices obtained from adult mammalian hearts mostly have been limited to 48 hours, which diminishes the usefulness of the preparation for testing effect of chronic drug and gene therapies (Brandenburger et al., 2012; Bussek et al., 2012; Kang et al., 2016). Lacking pacemaking abilities, slices collected from the ventricles of the heart undergo significant dedifferentiation, when cultured with conventional tissue culture techniques that lack electrical or mechanical stimulation and loading (Brandenburger et al., 2012; Kaneko et al., 2012). Human tissue and primary cells have been implemented in numerous body-on-a-chip systems designed for drug testing (Esch, Ueno, Applegate, & Shuler, 2016; Loskill et al., 2017; Phan et al., 2017). However, due to difficulties in maintaining the mature phenotype of adult human cardiac tissue *in vitro*, thus far there has not been a heart-on-a-chip system that supports long term organotypic culture of the human cardiac tissue. To achieve long-term culture of human cardiac slices while maintaining adult cardiomyocyte phenotype, we have developed a human-heart-on-a-chip system for organotypic culture of human cardiac tissue slices. The culture system supports media circulation, oxygenation, temperature control, electrical stimulation, and mechanical loading. The system is also entirely self-contained to allow for the transport of live cardiac slices to share for scientific research and drug testing.

4.2 Methods

4.2.1 Human cardiac slice preparation

Procurement of human cardiac tissue and procedures for obtaining viable human cardiac slices were described in Chapter 3.2.1 and 3.2.2. Experimental protocols were approved by the

George Washington University Institutional Review Board and were in accordance with human research guidelines.

4.2.2 Isolation of murine atrial preparation

Procedures for isolating murine atria for culture were discussed in Chapter 3.2.7. Mice were anesthetized in accordance with animal protocol approved by the George Washington University IACUC.

4.2.3 Optical mapping of human cardiac slices

Methods for optical mapping of human cardiac slices and data analysis were described previously in Chapter 3.2.4 and 3.2.5.

4.2.4 ECG data analysis

A custom MATLAB program (Fig. 4.5) was used to analyze the pseudo ECG recorded from the culture chambers. First, the signals were filtered with a 60Hz notch filter to remove the 60-cycle noise. The signal was then filtered with a 5th order band-pass Butterworth filter with a lower cutoff frequency at 5Hz and a higher cutoff frequency at 100Hz before peak detection was performed on the signal for heart rate calculation.

4.2.5 Microcontroller-controlled slice culture system

Custom electromechanical components were developed and fabricated to monitor and control the fundamental culture conditions, including media circulation, temperature adjustment, medium oxygenation, electrical stimulation, optical stimulation, and ECG recording. A

microcontroller (Teensy 3.2, PJRC, Sherwood, OR) was used to monitor and actively control each component of the system. The microcontroller interfaced with the rest of the system via a custom breakout board. To achieve medium circulation, we prototyped a peristaltic pump using 3D printing technique to achieve the appropriate flow rate with low power consumption. To maintain medium temperature and oxygenation, we fabricated a gas-exchanger with built in thermofoil heater (Minco, Minneapolis, MN) using a 3-axis CNC mill (Roland DGA, Irvine, CA). Since a 5.5 V battery was used to power the entire system, a voltage boost regulator (LMR62010, Texas Instrument, Dallas, TX) was used to drive the heater at 12V. A gas permeable PDMS sheet separated the oxygen from the culture medium. A humidity and temperature sensor (HTU21D, SparkFun, Boulder, CO) was mounted onto the thermofoil heater to prevent overheating of the culture medium and to detect system leakage.

Each tissue chamber is instrumented with an array of sensors and actuators to monitor the culture condition and stimulate the tissue to minimize dedifferentiation. To monitor the temperature inside the culture chambers, a high-precision platinum temperature sensor (Digikey, Thief River Falls, MN) was embedded into each chamber. The temperature signal was digitized by a high-precision analog-to-digital converter (ADS1220, Texas Instrument, Dallas, TX) and recorded by the microcontroller. Using the culture chamber temperature, a negative feedback control loop is used to control the heaters to actively maintain a stable culture medium temperature. To record far-field pseudo ECG of cultured tissue, silver/silver chloride sensing electrodes were fabricated into the culture chambers. The pseudo ECG was amplified 1000 times with an operational amplifier, and digitized via a multichannel high sampling rate analog-to-digital converter (ADS131A04, Texas Instrument, Dallas, TX). The ECG data was recorded by the microcontroller at 2kHz sampling rate for further processing. Electrical stimulation of the

slices is achieved with field stimulation via platinum/iridium electrodes. For optical stimulation of the cultured optogenetic tissue, a 470±10 nm LED (Wurth Electronics, Niedernhall, Germany) was built into each well. All mechanical components were designed in AutoCAD and fabricated with a 3D printer, a laser cutter, and a 3-axis CNC mill.

4.2.6 Statistical analysis

All data presented here are shown as mean ± standard deviation. The statistical analysis was performed using one-way ANOVA followed by a Dunnett's multiple comparisons test.

4.3 Results

With preserved extracellular matrix and native cell-cell coupling, vibratome-cut human cardiac slices have been demonstrated as an authentic model of the adult human heart for physiological studies and pharmacological testing (Brandenburger et al., 2012; Camelliti et al., 2011; Kang et al., 2016). We have previously established a protocol for obtaining viable human cardiac slices from non-failing donor hearts that were rejected for transplantation and from end-stage failing hearts (Kang et al., 2016). In this project, we further optimized the culture condition to extend viability length of the cardiac slices *in vitro*. Using optical mapping, we evaluated the conduction parameters of the culture cardiac slices. To achieve long-term culture of human cardiac slices, we developed an automated heart-on-a-chip system for organotypic culture of cardiac slices that supports electrical stimulation to minimize tissue dedifferentiation. The system is also entirely self-contained to allow for shipping of live human cardiac tissue.

4.3.2 Heart-on-a-chip system

To prolong the culture period of human cardiac slices and prevent tissue dedifferentiation, we developed a heart-on-a-chip electronic and microfluidic system for organotypic culture of human cardiac slices *in vitro*, as shown in Figure 4.1. The culture system continuously monitors and maintains stable culture conditions, including culture medium temperature, circulation, and oxygenation. The culture chambers include actuators and sensors for electrical stimulation, sensing, and optical stimulation. Unlike cell lines that could be cryopreserved for shipping, live human cardiac slices are susceptible to hypoxia when not maintained properly, thus complicating shipping of live slices across the country or internationally. The culture system that we developed is also fully self-contained with integrated power supply, oxygen source, and media reservoir, allowing the maintenance of tissue viability during transportation. To increase culture capacity and reduce the cost of repair, we designed the culture system to be modular for plug and play operation.

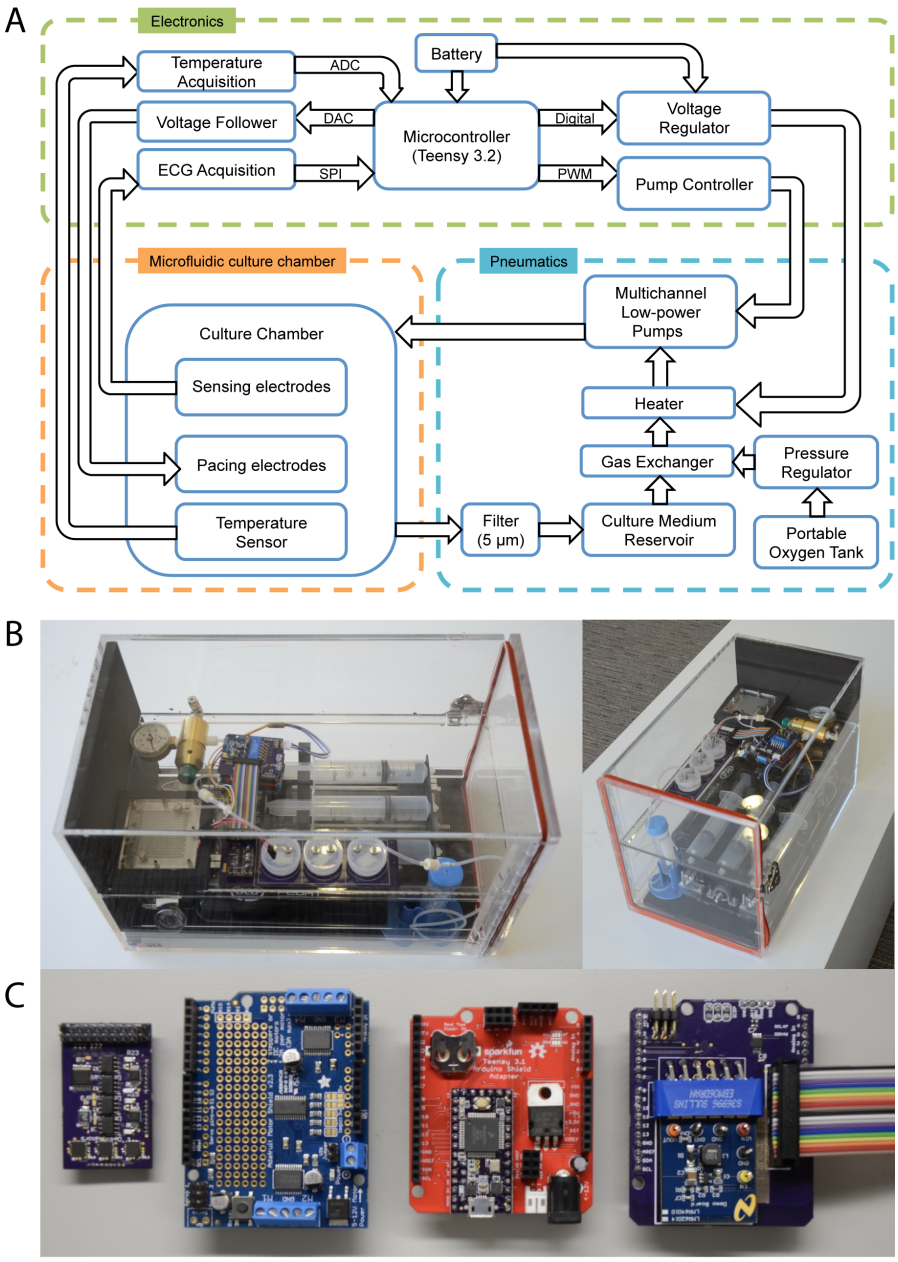

Figure 4.1 Human heart-on-a-chip system. A) Block diagram of the culture system. The system consists of custom electronics and electromechanical components to maintain stable culture conditions. B) Pictures of the assembled system. Insulation foam was removed from the sides of the enclosure for illustration. C) Modular electronic control unit. The electronic components consist of an acquisition module, a motor driver, a microcontroller, and a power module (from left to right).

The culture conditions inside the heart-on-a-chip system are closely monitored and adjusted by an array of sensors and actuators controlled by a microcontroller, as shown in Figure 4.1A. The system consists of a custom control module, multiple culture chambers, pumps,

heaters, a gas exchanger, a culture medium reservoir, a gas pressure regulator, and an oxygen tank. With an average current draw of below 600mA, the culture system has an operation time of three days on a single portable 40,000 mAh battery, which is sufficient for over-night shipping. All culture parameters can be independently adjusted in real time to determine and maintain the optimal culture condition for human cardiac slices.

4.3.3 Smart tissue culture chamber

Electrical stimulation has been shown to maintain the structural and functional properties of isolated adult rat ventricular myocytes(Berger et al., 1994; Folliguet et al., 2001). To minimize tissue dedifferentiation and to monitor the culture parameters, we instrumented each culture chamber with an array of actuators and sensors, including field-pacing electrodes, sensing electrodes, a temperature sensor, and a light source for optogenetic stimulation and fluorescence recordings (Fig. 4.2 B). The chamber bottoms are coated with polydimethylsiloxane (PDMS) for mechanical anchoring of the slices using miniature dissection pins. To avoid physical damage to the slice from point pacing electrodes, platinum-iridium (Pt/Ir) electrodes, which have proven biocompatibility and low electrical resistance, are fabricated into the culture chamber for field stimulation. The default stimulation parameters are set at 3V pulse amplitude, 2 ms pulse duration, and 1 second pacing cycle length. As shown in Figure 4.2 D, no undesirable voltage fluctuations were observed in the recorded stimulation waveform. The pacing parameters are user or software adjustable to allow for optimization of the pacing protocol during culture in case of changes in pacing threshold or specific protocol requirements.

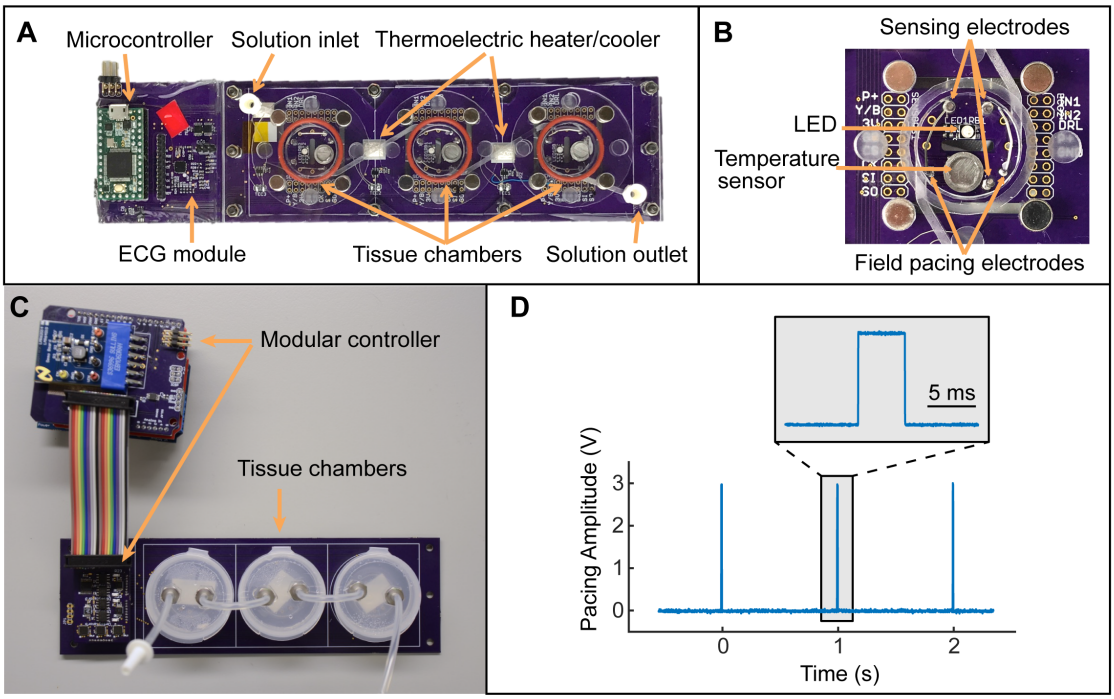

Figure 4.2 Smart tissue culture chamber. A) A fully integrated culture device for compactness. B) Culture chambers are instrumented with sensing electrodes, field pacing electrodes, a temperature sensor, and a LED. C) Modular culture system for each of scaling up culture capacity. D) Recorded waveform during electrical field stimulation with 3V pulse amplitude, 5ms pulse duration, and 1 second pacing cycle length.

Temperature of the culture medium is maintained by a feedback control system based on the temperature inside the chamber via a platinum resistance thermometer. Based on platinum's linear resistance-temperature relationship, an analog temperature signal is obtained by comparing the voltage from the platinum thermometer to a reference voltage with an instrumentation amplifier. The analog signal is then digitized with an analog to digital converter before being recorded and converted to Celsius by the microcontroller. We developed two configurations of the culture chambers, as shown in Figure 4.2 A, C. While both configurations perform similarly, the design shown in Figure 4.2 A is much more compact, with all electronic components integrated onto the same printed circuit board, whereas the system in Figure 4.2 C utilizes a modular design for the ease of scaling up culture capacity with plug and play operation.

Due to the scarcity of human heart tissue, isolated murine atrial preparation containing sinus node was used to test and optimize the culture system during development. Viability of the culture murine atrial preparation was measured by the intrinsic heart rate of the sinus node. To monitor the murine atrial sinus rhythm in culture, we fabricated Pt/Ir sensing electrodes into the culture chambers for pseudo ECG recording. The pseudo ECG was amplified 1,000x with an operational amplifier and digitized via a multichannel high sampling rate analog-to-digital at 2kHz sampling rate. The ECG data was recorded by the microcontroller for post processing.

4.3.4 Custom gas exchanger

Since the thickness of human cardiac slices approaches the limit of oxygen diffusion, sufficient oxygenation of the culture medium is critical to maintaining tissue viability (Barclay, 2005). When cultured in a regular incubator with 20% O_2, the core of the tissue slice may experience hypoxia, causing altered gene expression and reducing tissue viability (Giordano, 2005; Huang, 2004). To supply sufficient oxygen to the slices, a custom gas exchanger was developed to oxygenate the culture medium before it is circulated to the culture chambers, as shown in Figure 4.3 A. The gas exchanger consists of two mirrored chambers separated by a 0.35mm thick gas-permeable PDMS membrane. One chamber of the gas exchanger is pressurized with pure oxygen at 15psi, while the culture medium flows through the mirrored chamber. The total oxygen exchange surface is 17cm^2. Using an oxygen sensor (ADInstruments, Colorado Springs, CO), we measured a dissolved oxygen concentration of 1.3 mM in the culture medium, 5-6 times higher than that of conventional culture in a cell incubator (McMurtrey, 2016). As shown in Figure 4.3 E, gas exchange occurs rapidly inside the culture system. When the gas exchanger was filled with pure oxygen, the diffused oxygen level reached saturation in

approximately 15 minutes. Vice versa, when the oxygen was purged and nitrogen was fed into the gas exchanger, the oxygen concentration in the culture medium was depleted in approximately 15 minutes. To maintain tissue viability during transportation, the culture system also contains a portable small gas tank and a miniature pressure regulator (Fig. 4.3 C). The gas tank can be pressurized to 2100 psi, allowing for an estimated 3 weeks of oxygen supply.

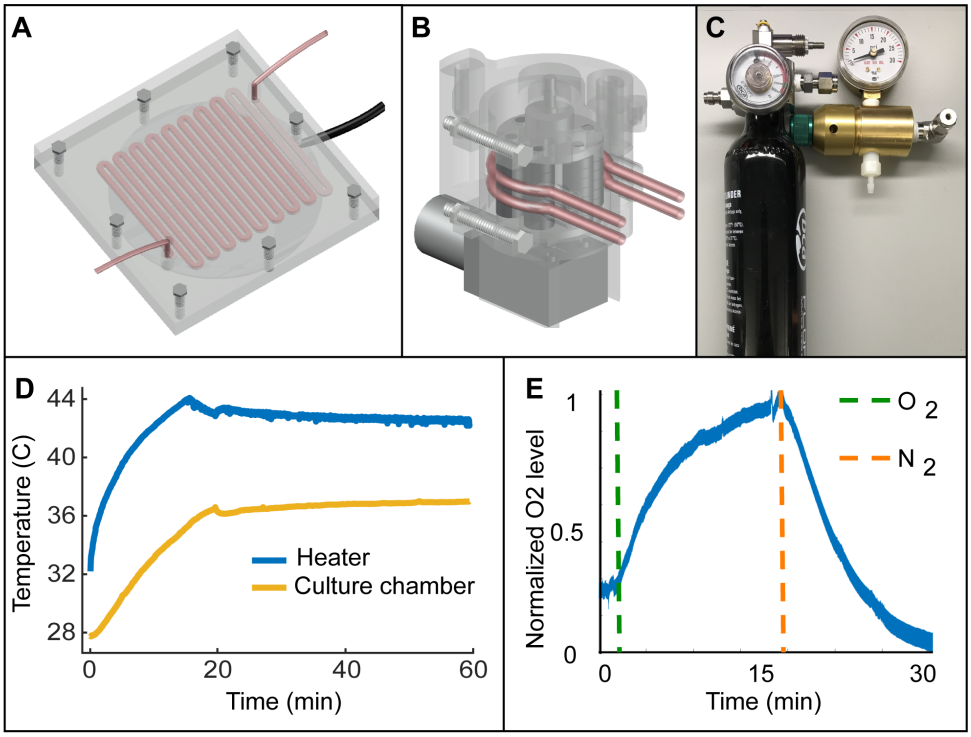

Figure 4.3 Custom gas exchanger, heater, and pump for maintaining culture medium oxygenation, temperature, and circulation. A) Rendering od the CNC milled gas exchanger. The top chamber is made of polycarbonate for liquid medium to pass through. The bottom chamber is made of stainless steel and is heated with a thermofoil heater. B) Rendering of the 3D printed peristaltic pump. C) Portable gas tank and miniature pressure regulator. D) Recorded temperatures of the heater and the culture chamber. The culture chamber temperature rapidly reaches and maintained physiological temperature with minimal fluctuation. E) Dissolved oxygen level in culture medium with different gas. The oxygen concentration in the liquid medium rapidly reached saturation when the gas exchanger is filled with oxygen. The dissolved oxygen was depleted when the gas exchanger was filled with nitrogen.

4.3.5 Maintenance of stable culture temperature

Since most enzymes denature rapidly at high temperatures and ion channel conductance is temperature dependent, the ability to maintain stable temperature inside the culture chambers is critical for preserving viability and normal electrophysiology of cardiac slices (Dumaine et al., 1999; Milburn, Saint, & Chung, 1995; Voets et al., 2004). We implemented a proportional control, a type of feedback control system, to maintain a stable culture medium temperature and to compensate for changing ambient temperature. Two thermofoil heaters were built into the gas exchanger and the medium reservoir, where the liquid medium has the greatest surface-to-volume ratio. Since heat transfer to the culture medium does not stop immediately when the heaters are powered off due to the large heat capacitance of the heaters, a proportional control system was implemented to avoid undesirable temperature fluctuations in the culture chambers, as shown in the following equation. To prevent overheating of the culture medium, the temperature of the heaters is monitored and limited to a maximum of 45°C, well below the inactivation temperature of fetal bovine serum. As shown in Figure 4.3 D, the culture medium inside the culture chamber reached 37°C from room temperature within 20 minutes with minimal overshoot. The temperature was subsequently maintained without fluctuations.

$$P_{out} = K_p\, e(t) + p0 \qquad (4.1)$$

Equation for proportional control, where p0 is output with zero error and is set at 37°C, e(t) is the instantaneous error at time t and is the difference between p0 and culture chamber temperature, K_p is a proportional gain and is set at 1, P_{out} is the target temperature of the heater. The upper bound of P_{out} is set to 45°C to avoid overheating of the culture medium.

4.3.6 Low-power pump for medium circulation

Both heating and oxygenation of the culture media require circulation of the perfusion medium. A robust means of driving steady flow is critical for maintaining stable heat and gas exchange. We evaluated several pumps for their long-term dependability and low power consumption, and adopted a piezoelectric pump and a custom peristaltic pump for two different versions the culture system. With a low power consumption of 250mW, the piezoelectric pump is preferred when power is limited, such as during transportation of the culture system. However, since the piezoelectric pump works by rapidly deforming and releasing a piezo element when voltage is applied at a high frequency, the pump requires direct contact with the culture medium and can potentially increase the chance of contamination. For the long-term culture of the cardiac slices when the culture system is connected to an external power source, we developed a custom 3D printed peristaltic pump as shown in Figure 4.3 B. Since the liquid is forced through a tube when compressed by rollers in a peristaltic pump, the tubing can be sterilized by ethylene oxide or autoclave to minimize the chance of contamination. With a power consumption of 1W, our custom peristaltic pump is 10-15 times more power efficient than similar commercially available pumps. With built-in reduction gears, our peristaltic pump is also significantly more reliable than other low cost peristaltic pumps that drive the rollers via friction coupling. To avoid excess pressure buildup in the gas exchanger, the piezoelectric pump and the peristaltic pump are controlled by pulse width modulation to achieve a stable 2mL/min flow rate.

4.3.7 Tissue viability in the heart-on-a-chip system

To evaluate the effectiveness of our culture system in maintaining viability of human cardiac slices, we performed optical mapping of the cardiac slices cultured in the system, and

tracked the automaticity of cultured murine atria. As a preliminary attempt to minimize tissue dedifferentiation, the human cardiac slices were paced at 1Hz with 5ms pulse width for 10 minutes every hour. As shown in Figure 4.4 A-C, the human cardiac slices cultured in the heart-on-a-chip system remained electrically viable for up to 3 days. When compared with a freshly sectioned slice (Fig. 4.4 A), the slices cultured for 1 day (Fig. 4.4 B) and 3 days (Fig. 4.4 C) demonstrated preserved anisotropic conduction and normal action potential morphology (Fig. 4.4 D). Greater noise was observed in the optical action potential recorded from the human cardiac slice cultured for 3 days, suggesting declining tissue viability. To achieve long-term culture of human cardiac slices, more optimization need to be performed in terms of the medium flow rate, oxygenation, medium composition, and the electrical stimulation protocol, which are all easily adjustable with our culture system.

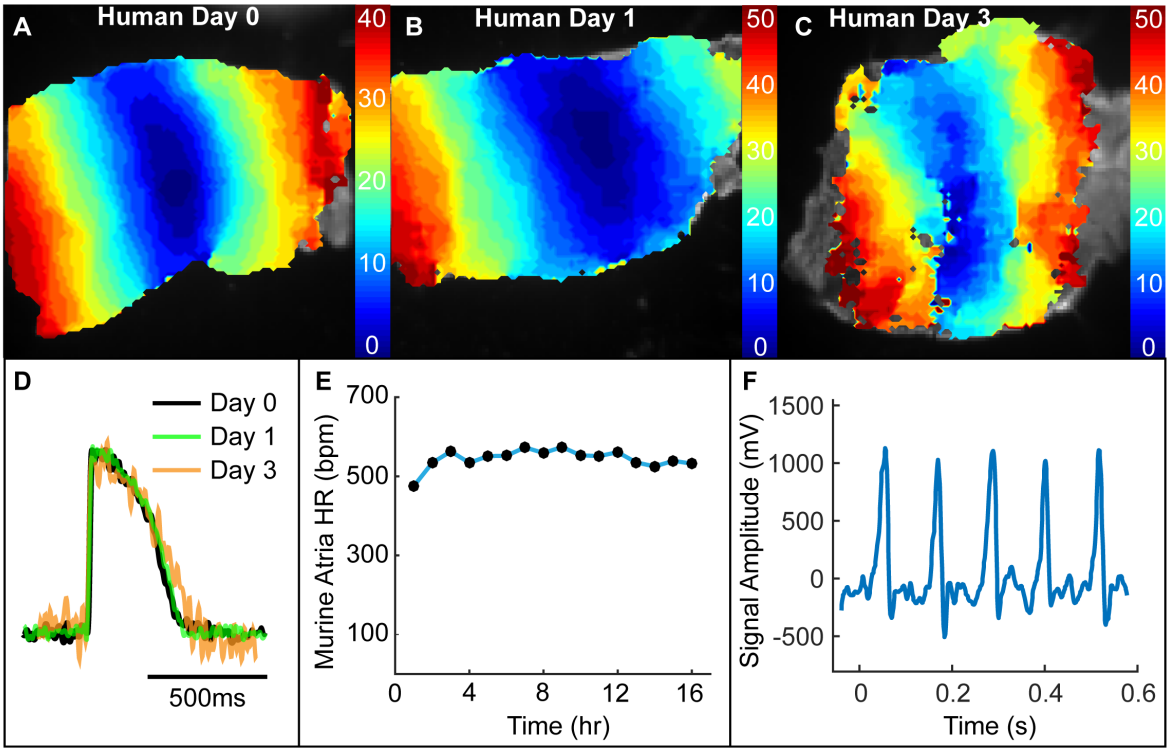

Figure 4.4 Organotypic culture of human and murine cardiac tissue in the heart-on-a-chip system. A-C) Activation maps of an acute human cardiac slice and slices cultured for 1 and 3 days in the culture system. The colorbars

represent activation times in ms. D) Action potential recorded from the slices using optical mapping. E) The heart-on-a-chip system maintained stable heart rate of the culture murine atrial preparation. F) Far-field recording of cultured murine atrial preparation.

Isolated murine atrial preparation has been used to study atrial conduction and pacemaking (Choate & Feldman, 2003; Glukhov, Flagg, Fedorov, Efimov, & Nichols, 2010; Swaminathan et al., 2011). The preparation can also be maintained in culture for extended period due to the thickness of the tissue. During development of the culture system, isolated murine atrial preparation was used to test the culture system. Since the sinoatrial node is preserved on the preparation, automaticity of the murine atria can be tracked as a measure of tissue viability. As shown in Figure 4.4 E, the cultured murine atria exhibited stable physiological heart rate in the culture system. To reduce motion artifacts in the far-field electrical recording, the system was programmed to power down medium circulation and heating during recording. As shown in Figure 4.4 F, a clean atrial electrical signal could be recorded for heart rate calculation.

We developed custom MATLAB program and a graphic user interface (GUI) to monitor the performance of the culture chamber and the condition of culture murine atria, as shown in Figure 4.5. The top panel in the GUI shows the temperatures of the heaters and the culture chambers over time for tracking heater and pump malfunction. The bottom 3 panels show far-field electrical recordings from the culture chambers. The recorded signal was filtered by a 2^{nd} order Butterworth notch filter to remove the 60Hz power line interference and a 5^{th} order band-pass Butterworth filter with a lower cutoff frequency at 5Hz and a higher cutoff frequency at 100Hz to remove drift and additional noise in the signal. Peak detection with user selectable settings can be performed on the electrical recordings for heart rate calculation.

Figure 4.5 Custom monitoring and analysis software. The main graphical user interface consists of 4 sections. Section 1 is for loading the device log and for selecting ECG recordings. Section 2 shows a history of the device temperature. Section 3 shows the psudo ECG recorded from the culture chambers. Section 4 is used for performing heart rate calculation with user selectable peak detection parameters.

4.4 Discussion

Previously, we demonstrated the advantages of human cardiac slices as a model for studying human cardiac physiology and for drug efficacy and toxicity testing (Kang et al., 2016). However, the limited culture duration and the intricate culture protocol impeded the use of human cardiac slices for long-term studies. Here, we developed an automated, self-contained heart-on-a-chip system for maintaining tissue viability and for transporting live tissue.

To achieve long-term culture of human cardiac slices while preserving normal physiology, we developed a heart-on-a-chip system in which different culture parameters can be individually adjusted to establish the optimal culture condition. We also designed our system to be entirely self-contained to support shipping of live cardiac slices. Using preset parameters and a feedback control system, the culture system maintains stable temperature, circulation, and oxygenation of the culture medium. The culture chambers are instrumented with an array of actuators and sensors for electrical stimulation, mechanical anchoring, electrical recording, and optogenetic stimulation and sensing.

Continual stimulation of isolated adult rat cardiomyocytes was found to preserve contractility, evident by the preserved amplitude of contraction, the velocities of shortening and relaxation, and the peak calcium current density (Berger et al., 1994). In the field of tissue engineering, electrical stimulation was also shown to improve expression of major cardiac markers and induced cell alignment and coupling in hiPSC-CMs (Radisic et al., 2004). With built-in field pacing electrodes, our culture system allows for testing of electrical stimulation protocols with different frequencies and durations to establish the optimal protocol for minimizing tissue dedifferentiation. Pt/Ir was chosen as the material for the pacing electrodes to avoid release of free radicals that could cause oxidative stress to the tissue. Any proton gradient generated by the electrical field would be dissipated by the circulation of the culture medium. In extreme cases where continuous high frequency pacing might be required to maintain tissue phenotype, electrolysis of the culture medium would break down sodium chloride and water molecules to form sodium hydroxide, causing an increase in pH of the culture medium. A collaborative effort to develop a miniature pH sensor with minimal baseline drift is underway.

The addition of a pH sensor will allow for real-time adjustment of the culture medium pH in near future.

To maintain a stable temperature in the culture system, we evaluated the effectiveness of three types of feedback control systems, including on-off control, proportional control, and proportional-integral-derivative (PID) control. Also known as a hysteresis controller, an on-off controller rapidly switches the power state of the heaters based on the temperature inside the culture chambers and is the easiest to implement. However, the on-off controller does not compensate for the delayed heat exchange between the heaters and the culture medium, causing large temperature oscillations. On the other hand, a PID controller can achieve stable temperature control for a given system configuration when the proportion, integral, and derivative terms are well characterized. However, the stringentness of a PID controller hinders its ability to adjust to changing system configurations. Therefore, the proportional controller was implemented in our culture system to achieve a stable temperature while allowing for plug and play operation of the culture chambers when expanding the culture capacity.

Here, we developed an automated, self-contained heart-on-a-chip system that maintains optimal condition for organotypic culture of human cardiac slices while providing electrical stimulation and mechanical anchoring for minimizing tissue dedifferentiation. The development of this culture system along with the human cardiac slice platform would accelerate pre-clinical drug testing and research in human cardiac physiology.

4.5 Acknowledgement

We are grateful to the Washington Regional Transplant Community and the families of donors. We also thank all members of the Efimov lab and the Kay Lab at George Washington

University, especially Dr. Chaoyi Kang, Jaclyn Brennan, Dr. Sharon George, Dr. Kedar Aras, Dr. Rokhaya Faye, and Frederick Zasadny for critical discussion of the project. We are grateful to Dr. Stacey Rentschler and Dr. Nathaniel Huebsch for their expert technical advice. This project was funded by National Institutes of Health (grants R01 HL114395 and R01 HL126802) and the Leducq Foundation (grant RHYTHM).

Chapter 5: Summary and future directions

Disruption in the transcriptional signaling pathways has been implicated in the pathogenesis of cardiac arrhythmia. To delineate one of the potential mechanisms of sick sinus syndrome and atrial fibrillation, I presented the extent of electrical remodeling in mice following a transient reactivation of Notch. The result of the study demonstrated that the transient reactivation of Notch in adult animals leads to prolonged sinus bradycardia, frequent sinus pauses, slow heterogeneous conduction, and an increased susceptibility to AF, as a result of the altered expression of several key regulators of conduction and pacemaking. To bridge the gap between bench research and human clinical therapy, I presented the prolonged culture of human cardiac slices as an accurate model of the human heart for research and drug testing. With the optimized culture protocol, the human cardiac slices obtained from the left ventricular free wall remained electrically viable for up to 21 days *in vitro* and routinely maintained normal electrophysiology for up to 4 days. To further improve human cardiac slice culture for long-term studies, I also presented a self-contained heart-on-a-chip system for automated culture of human cardiac slices. The culture system maintains optimal culture conditions and provides electrical stimulation and mechanical anchoring to minimize tissue dedifferentiation. This work allows for accelerated optimization of long-term culturing of human cardiac slice, which will enable study of arrhythmia mechanisms on human cardiac tissue via targeted control of transcription factors.

5.1 Optimizing human slice culture condition

Tissue remodeling has been observed in several studies that attempted to establish long-term culture of cardiac slices and primary cardiomyocytes. In the absence of electrical and/or

mechanical stimulations, cardiomyocytes undergo significant remodeling and dedifferentiation, evident by diminished contractile force, triangulation of action potential morphology, and reduced gap junction expression (Brandenburger et al., 2012; Kaneko et al., 2012). On the other hand, excessive electrical stimulation without electromechanical uncoupling may result in mitochondrial hypoxia (Kuzmiak-Glancy et al., 2017a). Therefore, optimization of the programmed stimulation protocol is critical to minimizing tissue dedifferentiation in the long-term culture of human cardiac slices, evident by the slowed conduction velocity (Fig. 3.6). A key feature of the automated heart-on-a-chip system presented in Chapter 4 is that the pulse amplitude, pulse duration, pacing cycle length, and total duration of the pacing train can be easily programmed for individual culture chambers, allowing simultaneous comparison of multiple pacing parameters. The culture condition can be further optimized by introducing perfluorocarbon (PFC), a synthetic oxygen carrier, to the culture medium. PFC has been shown to increase the oxygen carrying capacity of liquid medium by 3.6-fold (Kuzmiak-Glancy et al., 2017b). With the addition of PFC, extended electrical stimulation may be implemented without electromechanical uncoupling, which allows for mechanical stimulation of the slices when anchored. The healthy myocardium has a stiffness measured around 10 kPa Young's modules (Engler et al., 2008). To simulate mechanical loading on the cardiac slices, we plan to use soft lithography to create PDMS pillars of appropriate stiffness as a substrate where the slices will be mounted using permeable hydrogel adhesives. During electrical stimulation, the cardiac slices will contract against these pillars of matching stiffness.

Appropriate oxygenation and pH of the culture medium is critical for maintaining normal cellular function (Davies, 1995; Orchard & Kentish, 1990). To achieve greater control of the culture conditions, we plan to implement feedback control systems that monitor and adjust the

oxygenation and pH of the culture medium. Typical flow-through oxygen and pH sensors are electrochemical sensors that are susceptible to baseline drift and require periodic calibration. With advancements in sensor technologies, we hope to achieve real-time monitoring and adjustment of medium oxygenation and pH by adding a portable CO_2 tank and changing the partial pressure of CO_2 and O_2 in the gas exchanger using electronically controlled gas valves.

5.2 Real-time multiparametric characterization of cultured human cardiac slices

To achieve automated testing of drugs, gene therapies, and gene editing, we plan to develop technologies for multiparametric functional characterization of cultured human cardiac slices, as illustrated in Figure 4.6. Building on our current heart-on-a-chip system, we plan to develop a microelectrode array system for real-time monitoring of CV and APD and a compact optical detection system for measuring transmembrane potential, intracellular calcium dynamics, and metabolic function. A major advantage of the optical mapping technique is its ability to measure multiple functional parameters simultaneously with careful selection of voltage and calcium sensitive fluorescent probes. An optical mapping system can be built on a motorized stage for automated functional characterization of the cultured slices. The tissue will be epi-illuminated with the light source built into each culture chamber. Appropriate dichroic mirrors and filters can be implemented into the optical mapping system for simultaneous recording of voltage-sensitive fluorescent probe, calcium-sensitive fluorescent probe, and NADH autofluorescence. Since the stiffness of the substrate that the slices are mounted on could be easily controlled, the imaging system can also be used to calculate the contractility of the

cultured slices by tracking the displacement of the contraction during electrical stimulation (Norman, Mukundan, Bernstein, & Pruitt, 2008).

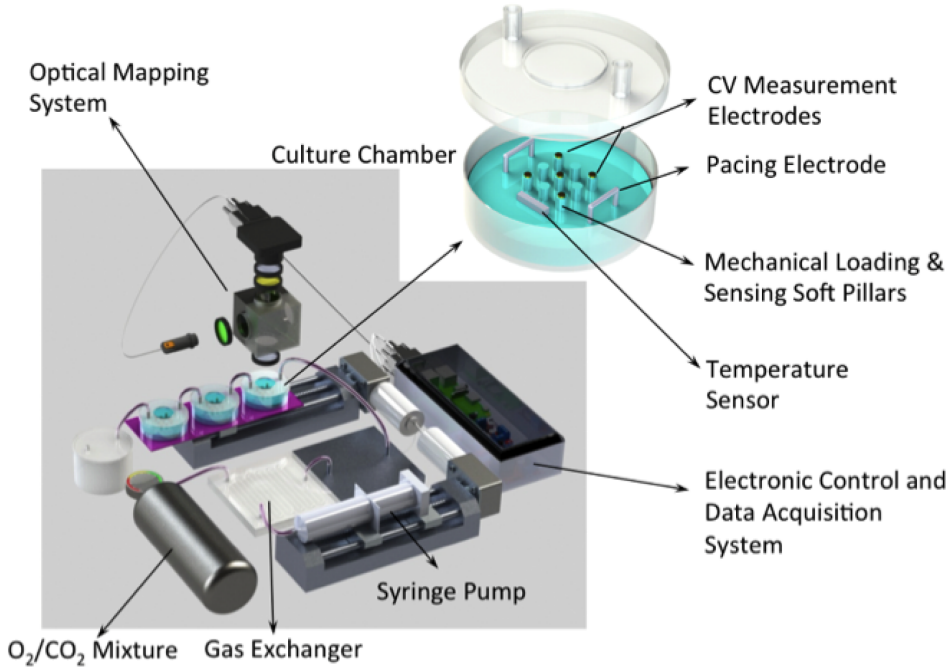

Figure 5.1 Future work on automated multiparametric characterization of cardiac slices. Miniaturized optical mapping system will be used for measuring action potential, calcium transient, and metabolic state of cultured slices on a motorized stage. A multi-electrode array system will be implemented in the culture chambers for real-time functional monitoring of the slices.

To increase the spatial specificity of stimulation and sensing inside the culture chambers of the heart-on-a-chip system, previously developed high-density actuators and sensors on a flexible and stretchable circuit could be implemented (Gutbrod, Sulkin, Rogers, & Efimov, 2014). The actuators and sensors include pacing electrodes, pH sensor, temperature sensor, ECG sensor, and strain gauge. The flexibility of the conformal circuits allows for real-time high-resolution electrogram mapping of the cultured slices with minimal motion artifact. To mount the cardiac slices to the conformal electronics inside the culture chambers, a suitable adhesive with appropriate biocompatibility, conductivity, and permeability is required. Chitosan-based adhesive is becoming a promising biomaterial for tissue repair and regenerative medicine

(Martins et al., 2014; Mihic et al., 2015; Yamada et al., 2000). The polymer hydrogel has been shown to have no cyctotoxicity to cardiomyocyte culture, support electrical coupling, and stable in water-based solutions. Different biocompatible adhesives including the chitosan-based adhesive should be evaluated for use in maintaining human cardiac slice culture.

The development of a heart-on-a-chip system with automated multiparametric characterization would accelerate pre-clinical drug testing and research in human cardiac physiology. In addition, integration of heart-on-a-chip with other human organ tissue slices and/or human iPSC derived cell/tissues would enable physiological investigations on a human-on-a-chip system. The development of the heart-on-a-chip technology presented here further facilitates the use of organotypic human cardiac slices as a platform for pre-clinical drug testing and research in human cardiac physiology.

References

Arnolds, D. E., Liu, F., Fahrenbach, J. P., Kim, G. H., Schillinger, K. J., Smemo, S., … Moskowitz, I. P. (2012). TBX5 drives Scn5a expression to regulate cardiac conduction system function. *Journal of Clinical Investigation*, *122*(7), 2509–2518. https://doi.org/10.1172/JCI62617

Bagwe, S., Berenfeld, O., Vaidya, D., Morley, G. E., & Jalife, J. (2005). Altered right atrial excitation and propagation in connexin40 knockout mice. *Circulation*, *112*(15), 2245–2253. https://doi.org/10.1161/CIRCULATIONAHA.104.527325

Barclay, C. J. (2005). Modelling diffusive O2 supply to isolated preparations of mammalian skeletal and cardiac muscle. *Journal of Muscle Research and Cell Motility*, *26*(4–5), 225–235. https://doi.org/10.1007/s10974-005-9013-x

Berger, H. J., Prasad, S. K., Davidoff, A. J., Pimental, D., Ellingsen, O., Marsh, J. D., … Kelly, R. A. (1994). Continual electric field stimulation preserves contractile function of adult ventricular myocytes in primary culture. *The American Journal of Physiology*, *266*(1 Pt 2), H341-9. https://doi.org/10.1152/ajpheart.1994.266.1.H341

Bird, S. D., Doevendans, P. A., Van Rooijen, M. A., Brutel De La Riviere, A., Hassink, R. J., Passier, R., & Mummery, C. L. (2003). The human adult cardiomyocyte phenotype. *Cardiovascular Research*, *58*(2), 423–434. https://doi.org/10.1016/S0008-6363(03)00253-0

Brandenburger, M., Wenzel, J., Bogdan, R., Richardt, D., Nguemo, F., Reppel, M., … Dendorfer, A. (2012). Organotypic slice culture from human adult ventricular myocardium.

Cardiovascular Research, *93*(1), 50–59. https://doi.org/10.1093/cvr/cvr259

Bray, M. a, Lin, S. F., Aliev, R. R., Roth, B. J., & Wikswo, J. P. (2001). Experimental and theoretical analysis of phase singularity dynamics in cardiac tissue. *Journal of Cardiovascular Electrophysiology*, *12*(6), 716–722. https://doi.org/10.1046/j.1540-8167.2001.00716.x

Bressan, M., Liu, G., & Mikawa, T. (2013). Early mesodermal cues assign avian cardiac pacemaker fate potential in a tertiary heart field. *Science*, *340*(6133), 744–748. https://doi.org/10.1126/science.1232877

Burnett, D., Abi-Samra, F., & Vacek, J. L. (1999). Use of intravenous adenosine as a noninvasive diagnostic test for sick sinus syndrome. *American Heart Journal*, *137*(3), 435–438. https://doi.org/10.1016/S0002-8703(99)70488-6

Bussek, A., Schmidt, M., Bauriedl, J., Ravens, U., Wettwer, E., & Lohmann, H. (2012). Cardiac tissue slices with prolonged survival for in vitro drug safety screening. *Journal of Pharmacological and Toxicological Methods*, *66*(2), 145–151. https://doi.org/10.1016/j.vascn.2011.12.002

Bussek, A., Wettwer, E., Christ, T., Lohmann, H., Camelliti, P., & Ravens, U. (2009). Tissue slices from adult mammalian hearts as a model for pharmacological drug testing. *Cellular Physiology and Biochemistry*, *24*(5–6), 527–536. https://doi.org/10.1159/000257528

Camelliti, P., Al-Saud, S. A., Smolenski, R. T., Al-Ayoubi, S., Bussek, A., Wettwer, E., … Terracciano, C. M. (2011). Adult human heart slices are a multicellular system suitable for electrophysiological and pharmacological studies. *Journal of Molecular and Cellular*

Cardiology, *51*(3), 390–398. https://doi.org/10.1016/j.yjmcc.2011.06.018

CDC. NCHS. (2015). Underlying Cause of Death 1999-2014 on CDC WONDER Online Database. Retrieved from http://wonder.cdc.gov/ucd-icd10.html

Chi, K. R. (2013). Revolution dawning in cardiotoxicity testing. *Nature Reviews Drug Discovery*, *12*(8), 565–567. https://doi.org/10.1038/nrd4083

Choate, J. K., & Feldman, R. (2003). Neuronal control of heart rate in isolated mouse atria. *American Journal of Physiology - Heart and Circulatory Physiology*, *285*(3), H1340–H1346. https://doi.org/10.1152/ajpheart.01119.2002

Coppini, R., Ferrantini, C., Aiazzi, A., Mazzoni, L., Sartiani, L., Mugelli, A., … Cerbai, E. (2014). Isolation and functional characterization of human ventricular cardiomyocytes from fresh surgical samples. *Journal of Visualized Experiments : JoVE*, (April), 1–14. https://doi.org/10.3791/51116

Corbel, S. Y., & Rossi, F. M. V. (2002). Latest developments and in vivo use of the Tet system: Ex vivo and in vivo delivery of tetracycline-regulated genes. *Current Opinion in Biotechnology*. https://doi.org/10.1016/S0958-1669(02)00361-0

Cox, J. L., Schuessler, R. B., & Boineau, J. P. (2000). The development of the Maze procedure for the treatment of atrial fibrillation. *Seminars in Thoracic and Cardiovascular Surgery*. https://doi.org/10.1016/S1043-0679(00)70010-4

Davies, K. J. (1995). Oxidative stress: the paradox of aerobic life. *Biochemical Society Symposium*, *61*, 1–31. https://doi.org/10.1042/bss0610001

Davis, R. C., Hobbs, F. D., & Lip, G. Y. (2000). ABC of heart failure. History and epidemiology. *BMJ (Clinical Research Ed.)*, *320*(7226), 39–42. https://doi.org/10.1136/bmj.320.7226.39

de Boer, T. P., Camelliti, P., Ravens, U., & Kohl, P. (2009). Myocardial tissue slices: organotypic pseudo-2D models for cardiac research & development. *Future Cardiology*, *5*(5), 425–430. https://doi.org/10.2217/fca.09.32

De Sisti, A., Leclercq, J. F., Fiorello, P., Di Lorenzo, M., Manot, S., Halimi, F., & Attuel, P. (1999). Sick sinus syndrome with and without atrial fibrillation: atrial refractoriness and conduction characteristics. *Cardiologia*, *44*(4), 361–367. Retrieved from http://www.ncbi.nlm.nih.gov/pubmed/10371788

Dmitriev, I., Krasnykh, V., Miller, C. R., Wang, M., Kashentseva, E., Mikheeva, G., … Curiel, D. T. (1998). An adenovirus vector with genetically modified fibers demonstrates expanded tropism via utilization of a coxsackievirus and adenovirus receptor-independent cell entry mechanism. *Journal of Virology*, *72*(12), 9706–13. Retrieved from http://www.ncbi.nlm.nih.gov/pubmed/9811704%5Cnhttp://www.pubmedcentral.nih.gov/articlerender.fcgi?artid=PMC110480

Dobrzynski, H., Boyett, M. R., & Anderson, R. H. (2007). New insights into pacemaker activity: Promoting understanding of sick sinus syndrome. *Circulation*. https://doi.org/10.1161/CIRCULATIONAHA.106.616011

Doshi, A. N., Walton, R. D., Krul, S. P., de Groot, J. R., Bernus, O., Efimov, I. R., … Coronel, R. (2015). Feasibility of a semi-automated method for cardiac conduction velocity analysis

of high-resolution activation maps. *Computers in Biology and Medicine*, *65*, 177–183. https://doi.org/10.1016/j.compbiomed.2015.05.008

Dumaine, R., Towbin, J., Brugada, P., Vatta, M., Nesterenko, D. V, Nesterenko, V. V, … Antzelevitch, C. (1999). Ionic mechanisms responsible for the electrocardiographic phenotype of the Brugada syndrome are temperature dependent. *Circulation Research*, *85*(9), 803–809. https://doi.org/10.1161/01.RES.85.9.803

Efimov, I. R., Nikolski, V. P., & Salama, G. (2004). Optical imaging of the heart. *Circulation Research*. https://doi.org/10.1161/01.RES.0000130529.18016.35

Engler, A. J., Carag-Krieger, C., Johnson, C. P., Raab, M., Tang, H.-Y., Speicher, D. W., … Discher, D. E. (2008). Embryonic cardiomyocytes beat best on a matrix with heart-like elasticity: scar-like rigidity inhibits beating. *Journal of Cell Science*, *121*(22), 3794–3802. https://doi.org/10.1242/jcs.029678

Esch, M. B., Ueno, H., Applegate, D. R., & Shuler, M. L. (2016). Modular, pumpless body-on-a-chip platform for the co-culture of GI tract epithelium and 3D primary liver tissue. *Lab Chip*, *16*(14), 2719–2729. https://doi.org/10.1039/C6LC00461J

Fedorov, V. V., Glukhov, A. V., Ambrosi, C. M., Kostecki, G., Chang, R., Janks, D., … Efimov, I. R. (2011). Effects of KATP channel openers diazoxide and pinacidil in coronary-perfused atria and ventricles from failing and non-failing human hearts. *Journal of Molecular and Cellular Cardiology*, *51*(2), 215–225. https://doi.org/10.1016/j.yjmcc.2011.04.016

Ferrer, M. I. (1968). The Sick Sinus Syndrome in Atrial Disease. *JAMA: The Journal of the American Medical Association*, *206*(3), 645–646.

https://doi.org/10.1001/jama.1968.03150030101028

Fleck, T., Khazen, C., Wolner, E., & Grabenwoger, M. (2006). The incidence of reoperations in pacemaker recipients. *Heart Surgery Forum*, *9*(5), 306–309. https://doi.org/10.1532/HSF98.20061057

Folliguet, T. A., Rücker-Martin, C., Pavoine, C., Deroubaix, E., Henaff, M., Mercadier, J. J., & Hatem, S. N. (2001). Adult cardiac myocytes survive and remain excitable during long-term culture on synthetic supports. *Journal of Thoracic and Cardiovascular Surgery*, *121*(3), 510–519. https://doi.org/10.1067/mtc.2001.112528

Gahwiler, B. H., Capogna, M., Debanne, D., McKinney, R. A., & Thompson, S. M. (1997). Organotypic slice cultures: a technique has come of age. *Trends Neurosci*, *20*(10), 471–477. https://doi.org/S0166-2236(97)01122-3 [pii]

Giordano, F. J. (2005). Oxygen, oxidative stress, hypoxia, and heart failure. *Journal of Clinical Investigation*. https://doi.org/10.1172/JCI200524408

Glukhov, A. V., Fedorov, V. V., Kalish, P. W., Ravikumar, V. K., Lou, Q., Janks, D., … Efimov, I. R. (2012). Conduction remodeling in human end-stage nonischemic left ventricular cardiomyopathy. *Circulation*, *125*(15), 1835–1847. https://doi.org/10.1161/CIRCULATIONAHA.111.047274

Glukhov, A. V., Fedorov, V. V., Lou, Q., Ravikumar, V. K., Kalish, P. W., Schuessler, R. B., … Efimov, I. R. (2010). Transmural dispersion of repolarization in failing and nonfailing human ventricle. *Circulation Research*, *106*(5), 981–991. https://doi.org/10.1161/CIRCRESAHA.109.204891

Glukhov, A. V., Flagg, T. P., Fedorov, V. V., Efimov, I. R., & Nichols, C. G. (2010). Differential KATP channel pharmacology in intact mouse heart. *Journal of Molecular and Cellular Cardiology*, *48*(1), 152–160. https://doi.org/10.1016/j.yjmcc.2009.08.026

Govorunova, E. G., Sineshchekov, O. A., Janz, R., Liu, X., & Spudich, J. L. (2015). Natural light-gated anion channels: A family of microbial rhodopsins for advanced optogenetics. *Science*, *349*(6248), 647–650. https://doi.org/10.1126/science.aaa7484

Gude, N. A., Emmanuel, G., Wu, W., Cottage, C. T., Fischer, K., Quijada, P., … Sussman, M. A. (2008). Activation of Notch-mediated protective signaling in the myocardium. *Circulation Research*, *102*(9), 1025–1035. https://doi.org/10.1161/CIRCRESAHA.107.164749

Gutbrod, S. R., Sulkin, M. S., Rogers, J. A., & Efimov, I. R. (2014). Patient-specific flexible and stretchable devices for cardiac diagnostics and therapy. *Progress in Biophysics and Molecular Biology*. https://doi.org/10.1016/j.pbiomolbio.2014.07.011

Gutbrod, S. R., Walton, R., Gilbert, S., Meillet, V., Jaïs, P., Hocini, M., … Efimov, I. R. (2015). Quantification of the transmural dynamics of atrial fibrillation by simultaneous endocardial and epicardial optical mapping in an acute sheep model. *Circulation: Arrhythmia and Electrophysiology*, *8*(2), 456–465. https://doi.org/10.1161/CIRCEP.114.002545

Habeler, W., Peschanski, M., & Monville, C. (2009). Organotypic heart slices for cell transplantation and physiological studies. *Organogenesis*, *5*(2), 62–6. https://doi.org/10.4161/org.5.2.9091

Habeler, W., Pouillot, S., Plancheron, A., Puc??at, M., Peschanski, M., & Monville, C. (2009). An in vitro beating heart model for long-term assessment of experimental therapeutics.

Cardiovascular Research, *81*(2), 253–259. https://doi.org/10.1093/cvr/cvn299

Hanna, J., Markoulaki, S., Schroderet, P., Carey, B. W., Beard, C., Wering, M., … Jaenisch, R. (2008). Direct reprogramming of terminally differentiated mature B lymphocytes to pluripotency. *Cell*, *133*(2), 250–264. https://doi.org/10.1016/j.cell.2008.03.028

Hasenfuss, G. (1998). Animal models of human cardiovascular disease, heart failure and hypertrophy. *Cardiovascular Research*, *39*(1), 60–76. https://doi.org/10.1016/S0008-6363(98)00110-2

Hirt, M. N., Boeddinghaus, J., Mitchell, A., Schaaf, S., Börnchen, C., Müller, C., … Eschenhagen, T. (2014). Functional improvement and maturation of rat and human engineered heart tissue by chronic electrical stimulation. *Journal of Molecular and Cellular Cardiology*, *74*, 151–161. https://doi.org/10.1016/j.yjmcc.2014.05.009

Hong, J., Ku, S. H., Lee, M. S., Jeong, J. H., Mok, H., Choi, D., & Kim, S. H. (2014). Cardiac RNAi therapy using RAGE siRNA/deoxycholic acid-modified polyethylenimine complexes for myocardial infarction. *Biomaterials*, *35*(26), 7562–7573. https://doi.org/10.1016/j.biomaterials.2014.05.025

Huang, Y. (2004). Cardiac myocyte-specific HIF-1 deletion alters vascularization, energy availability, calcium flux, and contractility in the normoxic heart. *The FASEB Journal*. https://doi.org/10.1096/fj.04-1510fje

Itzhaki, I., Maizels, L., Huber, I., Zwi-Dantsis, L., Caspi, O., Winterstern, A., … Gepstein, L. (2011). Modelling the long QT syndrome with induced pluripotent stem cells. *Nature*, *471*(7337), 225–230. https://doi.org/10.1038/nature09747

Jia, Z., Valiunas, V., Lu, Z., Bien, H., Liu, H., Wang, H. Z., … Entcheva, E. (2011). Stimulating cardiac muscle by light cardiac optogenetics by cell delivery. *Circulation: Arrhythmia and Electrophysiology*, *4*(5), 753–760. https://doi.org/10.1161/CIRCEP.111.964247

Kaese, S., Frommeyer, G., Verheule, S., Van Loon, G., Gehrmann, J., Breithardt, G., & Eckardt, L. (2013). The ECG in cardiovascular-relevant animal models of electrophysiology. *Herzschrittmachertherapie Und Elektrophysiologie*, *24*(2), 84–91. https://doi.org/10.1007/s00399-013-0260-z

Kaneko, M., Coppen, S. R., Fukushima, S., Yacoub, M. H., & Suzuki, K. (2012). Histological Validation of Heart Slices as a Model in Cardiac Research. *Journal of Cell Science & Therapy*, *3*(4). https://doi.org/10.4172/2157-7013.1000126

Kang, C., Qiao, Y., Li, G., Baechle, K., Camelliti, P., Rentschler, S., & Efimov, I. R. (2016). Human Organotypic Cultured Cardiac Slices: New Platform For High Throughput Preclinical Human Trials. *Scientific Reports*, *6*. https://doi.org/10.1038/srep28798

Kapoor, N., Liang, W., Marbán, E., & Cho, H. C. (2013). Direct conversion of quiescent cardiomyocytes to pacemaker cells by expression of Tbx18. *Nature Biotechnology*, *31*(1), 54–62. https://doi.org/10.1038/nbt.2465

Karakikes, I., Ameen, M., Termglinchan, V., & Wu, J. C. (2015). Human Induced Pluripotent Stem Cell-Derived Cardiomyocytes: Insights into Molecular, Cellular, and Functional Phenotypes. *Circulation Research*. https://doi.org/10.1161/CIRCRESAHA.117.305365

Kehat, I., Khimovich, L., Caspi, O., Gepstein, A., Shofti, R., Arbel, G., … Gepstein, L. (2004). Electromechanical integration of cardiomyocytes derived from human embryonic stem

cells. *Nature Biotechnology*, *22*(10), 1282–1289. https://doi.org/10.1038/nbt1014

Kikuchi, K., McDonald, A. D., Sasano, T., & Donahue, J. K. (2005). Targeted modification of atrial electrophysiology by homogeneous transmural atrial gene transfer. *Circulation*, *111*(3), 264–270. https://doi.org/10.1161/01.CIR.0000153338.47507.83

Kiviniemi, M. S., Pirnes, M. A., Eränen, H. J. K., Kettunen, R. V. J., & Hartikainen, J. E. K. (1999). Complications related to permanent pacemaker therapy. *PACE - Pacing and Clinical Electrophysiology*, *22*(5), 711–720. https://doi.org/10.1111/j.1540-8159.1999.tb00534.x

KLEBER, A. G. (2004). Basic Mechanisms of Cardiac Impulse Propagation and Associated Arrhythmias. *Physiological Reviews*, *84*(2), 431–488. https://doi.org/10.1152/physrev.00025.2003

Kuzmiak-Glancy, S., Covian, R., Femnou, A. N., Glancy, B., Jaimes, R., Wengrowski, A. M., … Kay, M. W. (2017a). Cardiac performance is limited by oxygen delivery to the mitochondria in the crystalloid-perfused working heart. *American Journal of Physiology - Heart and Circulatory Physiology*, ajpheart.00321.2017. https://doi.org/10.1152/ajpheart.00321.2017

Kuzmiak-Glancy, S., Covian, R., Femnou, A. N., Glancy, B., Jaimes, R., Wengrowski, A. M., … Kay, M. W. (2017b). Cardiac performance is limited by oxygen delivery to the mitochondria in the crystalloid-perfused working heart. *American Journal of Physiology - Heart and Circulatory Physiology*, ajpheart.00321.2017. https://doi.org/10.1152/ajpheart.00321.2017

Lang, D., Holzem, K., Kang, C., Xiao, M., Hwang, H. J., Ewald, G. A., … Efimov, I. R. (2015). Arrhythmogenic remodeling of β<inf>2</inf> versus β<inf>1</inf> adrenergic signaling in the human failing heart. *Circulation: Arrhythmia and Electrophysiology*, *8*(2), 409–419. https://doi.org/10.1161/CIRCEP.114.002065

Lang, D., Sulkin, M., Lou, Q., & Efimov, I. R. (2011). Optical mapping of action potentials and calcium transients in the mouse heart. *Journal of Visualized Experiments : JoVE*, (55), e3275. https://doi.org/10.3791/3275

Laughner, J. I., Ng, F. S., Sulkin, M. S., Arthur, R. M., & Efimov, I. R. (2012). Processing and analysis of cardiac optical mapping data obtained with potentiometric dyes. *American Journal of Physiology. Heart and Circulatory Physiology*, *303*(7), H753-65. https://doi.org/10.1152/ajpheart.00404.2012

Lei, M., Goddard, C., Liu, J., Leoni, A. L., Royer, A., Fung, S. S., … Huang, C. L. (2005). Sinus node dysfunction following targeted disruption of the murine cardiac sodium channel gene Scn5a. *J Physiol*, *567*(Pt 2), 387–400. https://doi.org/10.1113/jphysiol.2005.083188

Lewis, T. (1925). *The Mechanism and Graphic Registration of the Heart Beat* (3rd ed.). London: Shaw & Sons.

Li, Y., Hiroi, Y., & Liao, J. K. (2010). Notch Signaling as an Important Mediator of Cardiac Repair and Regeneration After Myocardial Infarction. *Trends in Cardiovascular Medicine*. https://doi.org/10.1016/j.tcm.2011.11.006

Liu, H., Espinoza-Lewis, R. A., Chen, C., Hu, X., Zhang, Y., & Chen, Y. P. (2012). The role of Shox2 in SAN development and function. In *Pediatric Cardiology* (Vol. 33, pp. 882–889).

https://doi.org/10.1007/s00246-012-0179-x

Loskill, P., Sezhian, T., Tharp, K. M., Lee-Montiel, F. T., Jeeawoody, S., Reese, W. M., … Healy, K. E. (2017). WAT-on-a-chip: a physiologically relevant microfluidic system incorporating white adipose tissue. *Lab Chip*, *17*(9), 1645–1654. https://doi.org/10.1039/C6LC01590E

Lou, Q., Fedorov, V. V., Glukhov, A. V., Moazami, N., Fast, V. G., & Efimov, I. R. (2011). Transmural heterogeneity and remodeling of ventricular excitation- contraction coupling in human heart failure. *Circulation*, *123*(17), 1881–1890. https://doi.org/10.1161/CIRCULATIONAHA.110.989707

Lou, Q., Li, W., & Efimov, I. R. (2011). Multiparametric Optical Mapping of the Langendorff-perfused Rabbit Heart. *Journal of Visualized Experiments*, (55). https://doi.org/10.3791/3160

Lu, L., Mende, M., Yang, X., Körber, H.-F., Schnittler, H.-J., Weinert, S., … Ravens, U. (2012). Design and validation of a bioreactor for simulating the cardiac niche: a system incorporating cyclic stretch, electrical stimulation and constant perfusion. *Tissue Engineering Part A*, *19*, 120919081657001. https://doi.org/10.1089/ten.TEA.2012.0135

Maidhof, R., Tandon, N., Lee, E. J., Luo, J., Duan, Y., Yeager, K., … Vunjak-Novakovic, G. (2012). Biomimetic perfusion and electrical stimulation applied in concert improved the assembly of engineered cardiac tissue. *Journal of Tissue Engineering and Regenerative Medicine*, *6*(10). https://doi.org/10.1002/term.525

Mak, I. W. Y., Evaniew, N., & Ghert, M. (2014). Lost in translation: Animal models and clinical

trials in cancer treatment. *American Journal of Translational Research*. https://doi.org/1943-8141/AJTR1312010

Marsman, R. F., Tan, H. L., & Bezzina, C. R. (2014). Genetics of sudden cardiac death caused by ventricular arrhythmias. *Nature Reviews Cardiology*. https://doi.org/10.1038/nrcardio.2013.186

Martins, A. M., Eng, G., Caridade, S. G., Mano, J. F., Reis, R. L., & Vunjak-Novakovic, G. (2014). Electrically conductive chitosan/carbon scaffolds for cardiac tissue engineering. *Biomacromolecules*, *15*(2), 635–643. https://doi.org/10.1021/bm401679q

McMurtrey, R. J. (2016). Analytic Models of Oxygen and Nutrient Diffusion, Metabolism Dynamics, and Architecture Optimization in Three-Dimensional Tissue Constructs with Applications and Insights in Cerebral Organoids. *Tissue Engineering Part C: Methods*, *22*(3), 221–249. https://doi.org/10.1089/ten.tec.2015.0375

Mezzano, V., Liang, Y., Wright, A. T., Lyon, R. C., Pfeiffer, E., Song, M. Y., … Sheikh, F. (2016). Desmosomal junctions are necessary for adult sinus node function. *Cardiovascular Research*, *111*(3), 274–286. https://doi.org/10.1093/cvr/cvw083

Miake, J., Marbán, E., & Nuss, H. B. (2002). Gene therapy: Biological pacemaker created by gene transfer. *Nature*, *419*(6903), 132–133. https://doi.org/10.1038/419132b

Mihic, A., Cui, Z., Wu, J., Vlacic, G., Miyagi, Y., Li, S. H., … Li, R. K. (2015). A conductive polymer hydrogel supports cell electrical signaling and improves cardiac function after implantation into myocardial infarct. *Circulation*, *132*(8), 772–784. https://doi.org/10.1161/CIRCULATIONAHA.114.014937

Milburn, T., Saint, D. A., & Chung, S. H. (1995). The temperature dependence of conductance of the sodium channel: implications for mechanisms of ion permeation. *Receptors & Channels*, *3*(3), 201–211. Retrieved from http://www.ncbi.nlm.nih.gov/pubmed/8821793

Mines, G. R. (1913). On dynamic equilibrium in the heart. *The Journal of Physiology*, *46*(4–5), 349–383. https://doi.org/10.1113/jphysiol.1913.sp001596

Moreno, A., Kuzmiak-Glancy, S., Jaimes, R., & Kay, M. W. (2017). Enzyme-dependent fluorescence recovery of NADH after photobleaching to assess dehydrogenase activity of isolated perfused hearts. *Scientific Reports*, *7*. https://doi.org/10.1038/srep45744

Nadadur, R. D., Broman, M. T., Boukens, B., Mazurek, S. R., Yang, X., Van Den Boogaard, M., … Moskowitz, I. P. (2016). Pitx2 modulates a Tbx5-dependent gene regulatory network to maintain atrial rhythm. *Science Translational Medicine*, *8*(354). https://doi.org/10.1126/scitranslmed.aaf4891

Nakashima, Y., Yanez, D. A., Touma, M., Nakano, H., Jaroszewicz, A., Jordan, M. C., … Nakano, A. (2014). Nkx2-5 suppresses the proliferation of atrial myocytes and conduction system. *Circulation Research*, *114*(7), 1103–1113. https://doi.org/10.1161/CIRCRESAHA.114.303219

Nerbonne, J. M., Nichols, C. G., Schwarz, T. L., & Escande, D. (2001). Genetic manipulation of cardiac K(+) channel function in mice: what have we learned, and where do we go from here? *Circulation Research*, *89*(11), 944–56. https://doi.org/10.1161/hh2301.100349

Norman, J. J., Mukundan, V., Bernstein, D., & Pruitt, B. L. (2008). Microsystems for biomechanical measurements. *Pediatric Research*.

https://doi.org/10.1203/PDR.0b013e31816b2ec4

Orchard, C. H., & Kentish, J. C. (1990). Effects of changes of pH on the contractile function of cardiac muscle. *The American Journal of Physiology*, *258*(6 Pt 1), C967-81.

Park, D. S., & Fishman, G. I. (2011). The cardiac conduction system. *Circulation*. https://doi.org/10.1161/CIRCULATIONAHA.110.942284

Parrish, A. R., Gandolfi, A. J., & Brendel, K. (1995). Precision-cut tissue slices: Applications in pharmacology and toxicology. *Life Sciences*. https://doi.org/10.1016/0024-3205(95)02176-J

Phan, D. T. T., Wang, X., Craver, B. M., Sobrino, A., Zhao, D., Chen, J. C., … Hughes, C. C. W. (2017). A vascularized and perfused organ-on-a-chip platform for large-scale drug screening applications. *Lab Chip*, *17*(3), 511–520. https://doi.org/10.1039/C6LC01422D

Poller, W., Hajjar, R., Schultheiss, H. P., & Fechner, H. (2010). Cardiac-targeted delivery of regulatory RNA molecules and genes for the treatment of heart failure. *Cardiovascular Research*. https://doi.org/10.1093/cvr/cvq056

Psaty, B. M., Manolio, T. A., Kuller, L. H., Kronmal, R. A., Cushman, M., Fried, L. P., … Rautaharju, P. M. (1997). Incidence of and Risk Factors for Atrial Fibrillation in Older Adults. *Circulation*, *96*(7), 2455–2461. https://doi.org/10.1161/01.CIR.96.7.2455

Qu, Z., Xie, Y., Garfinkel, A., & Weiss, J. N. (2010). T-wave alternans and arrhythmogenesis in cardiac diseases. *Frontiers in Physiology*, *1 NOV*. https://doi.org/10.3389/fphys.2010.00154

Radisic, M., Park, H., Shing, H., Consi, T., Schoen, F. J., Langer, R., … Vunjak-Novakovic, G. (2004). Functional assembly of engineered myocardium by electrical stimulation of cardiac

myocytes cultured on scaffolds. *Proceedings of the National Academy of Sciences*, *101*(52), 18129–18134. https://doi.org/10.1073/pnas.0407817101

Rangarajan, S., Madden, L., & Bursac, N. (2014). Use of flow, electrical, and mechanical stimulation to promote engineering of striated muscles. *Annals of Biomedical Engineering*, *42*(7), 1391–1405. https://doi.org/10.1007/s10439-013-0966-4

Rentschler, S., Harris, B. S., Kuznekoff, L., Jain, R., Manderfield, L., Lu, M. M., … Epstein, J. A. (2011). Notch signaling regulates murine atrioventricular conduction and the formation of accessory pathways. *Journal of Clinical Investigation*, *121*(2), 525–533. https://doi.org/10.1172/JCI44470

Rentschler, S., Yen, A. H., Lu, J., Petrenko, N. B., Lu, M. M., Manderfield, L. J., … Epstein, J. A. (2012). Myocardial notch signaling reprograms cardiomyocytes to a conduction-like phenotype. *Circulation*, *126*(9), 1058–1066. https://doi.org/10.1161/CIRCULATIONAHA.112.103390

Robertson, C., Tran, D. D., & George, S. C. (2013). Concise review: Maturation phases of human pluripotent stem cell-derived cardiomyocytes. *Stem Cells*. https://doi.org/10.1002/stem.1331

Schmidt, R., & Nygren, A. (2006). Optical mapping system for visualizing arrhythmias in isolated mouse atria. In *Annual International Conference of the IEEE Engineering in Medicine and Biology - Proceedings* (pp. 4002–4005). https://doi.org/10.1109/IEMBS.2006.259600

Somasuntharam, I., Boopathy, A. V., Khan, R. S., Martinez, M. D., Brown, M. E., Murthy, N., &

Davis, M. E. (2013). Delivery of Nox2-NADPH oxidase siRNA with polyketal nanoparticles for improving cardiac function following myocardial infarction. *Biomaterials*, *34*(31), 7790–7798. https://doi.org/10.1016/j.biomaterials.2013.06.051

Suckau, L., Fechner, H., Chemaly, E., Krohn, S., Hadri, L., Kockskamper, J., … Poller, W. C. (2009). Long-term cardiac-targeted RNA interference for the treatment of heart failure restores cardiac function and reduces pathological hypertrophy. *Circulation*, *119*(9), 1241–1252. https://doi.org/10.1161/CIRCULATIONAHA.108.783852

Swaminathan, P. D., Purohit, A., Soni, S., Voigt, N., Singh, M. V., Glukhov, A. V., … Anderson, M. E. (2011). Oxidized CaMKII causes cardiac sinus node dysfunction in mice. *Journal of Clinical Investigation*, *121*(8), 3277–3288. https://doi.org/10.1172/JCI57833

Tandon, N., Cannizzaro, C., Chao, P.-H. G., Maidhof, R., Marsano, A., Au, H. T. H., … Vunjak-Novakovic, G. (2009). Electrical stimulation systems for cardiac tissue engineering. *Nature Protocols*, *4*(2), 155–173. https://doi.org/10.1038/nprot.2008.183

The FANTOM Consortium and the RIKEN PMI and CLST (dgt). (2014). A promoter-level mammalian expression atlas. *Nature*, *507*(7493), 462–470. https://doi.org/10.1038/nature13182

Thomas, C. E., Ehrhardt, A., & Kay, M. A. (2003). Progress and problems with the use of viral vectors for gene therapy. *Nat Rev Genet*, *4*(5), 346–358. https://doi.org/10.1038/nrg1066

Van Den Boogaard, M., Barnett, P., & Christoffels, V. M. (2014). From GWAS to function: Genetic variation in sodium channel gene enhancer influences electrical patterning. *Trends in Cardiovascular Medicine*. https://doi.org/10.1016/j.tcm.2013.09.001

Voets, T., Droogmans, G., Wissenbach, U., Janssens, A., Flockerzi, V., & Nilius, B. (2004). The principle of temperature-dependent gating in cold- and heat-sensitive TRP channels. *Nature*, *430*(7001), 748–754. https://doi.org/10.1038/nature02732

Wang, K., Lee, P., Mirams, G. R., Sarathchandra, P., Borg, T. K., Gavaghan, D. J., … Bollensdorff, C. (2015). Cardiac tissue slices: preparation, handling, and successful optical mapping. *American Journal of Physiology - Heart and Circulatory Physiology*, *308*(9), H1112–H1125. https://doi.org/10.1152/ajpheart.00556.2014

Wiener, N., & Rosenblueth, A. (1946). The mathematical formulation of the problem of conduction of impulses in a network of connected excitable elements, specifically in cardiac muscle. *Arch Inst Cardiol Mex*, *Jul*(3), 205–65.

Wiese, C., Grieskamp, T., Airik, R., Mommersteeg, M. T. M., Gardiwal, A., De Gier-De Vries, C., … Christoffels, V. M. (2009). Formation of the sinus node head and differentiation of sinus node myocardium are independently regulated by Tbx18 and Tbx3. *Circulation Research*, *104*(3), 388–397. https://doi.org/10.1161/CIRCRESAHA.108.187062

Yamada, K., Chen, T., Kumar, G., Vesnovsky, O., Topoleski, L. D. T., & Payne, G. F. (2000). Chitosan Based Water-Resistant Adhesive. Analogy to Mussel Glue. *Biomacromolecules*, *1*(2), 252–258. https://doi.org/10.1021/bm0003009

Yanger, K., Zong, Y., Maggs, L. R., Shapira, S. N., Maddipati, R., Aiello, N. M., … Stanger, B. Z. (2013). Robust cellular reprogramming occurs spontaneously during liver regeneration. *Genes and Development*, *27*(7), 719–724. https://doi.org/10.1101/gad.207803.112

Zhang, H., Zhao, Y., Lei, M., Dobrzynski, H., Liu, J. H., Holden, A. V., & Boyett, M. R. (2006).

Computational evaluation of the roles of Na+ current, iNa, and cell death in cardiac pacemaking and driving. *AJP: Heart and Circulatory Physiology*, *292*(1), H165–H174. https://doi.org/10.1152/ajpheart.01101.2005

Zhang, R., Han, P., Yang, H., Ouyang, K., Lee, D., Lin, Y. F., … Chi, N. C. (2013). In vivo cardiac reprogramming contributes to zebrafish hearT regeneration. *Nature*, *498*(7455), 497–501. https://doi.org/10.1038/nature12322